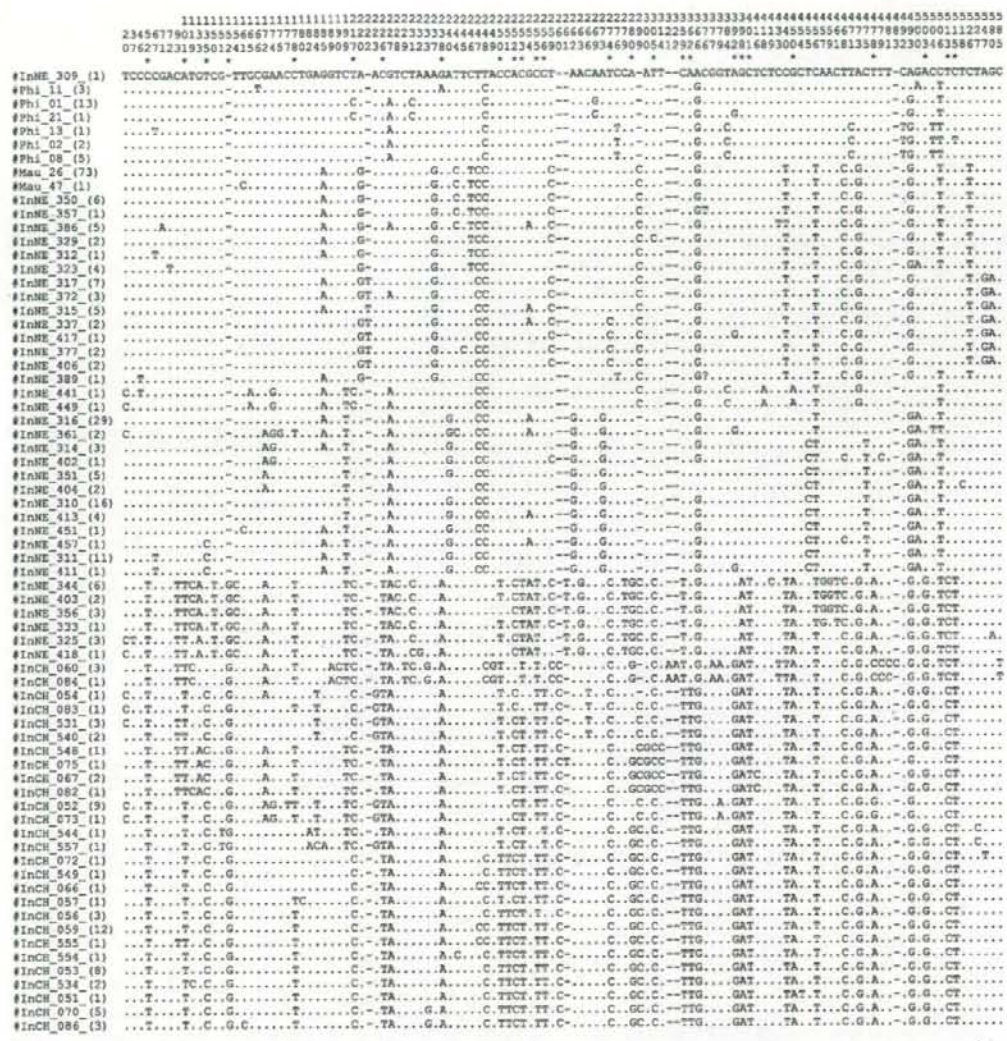

Figure 1. Variant sites of the mtDNA control region (HVII) in *Macaca fascicularis fascicularis* determined in this study. The sequence names begin with letters corresponding to the 4 populations (InCH = Indochina; InNE = Indonesia; Mau = Mauritius; and Phi = Philippines), followed by a code number identifying the sequence and a number in brackets corresponding to the number of animals sharing the sequence. Stars in the fourth line indicate the positions that differentiate Indochinese sequences from those of other populations.

Dating the Divergence of *Macaca fascicularis fascicularis* Populations

The Bayesian tree showing the length of branches (Figure 2) was transformed under the assumption of a constant rate of mutation, while keeping its tree topology, and the resulting tree is shown in Figure 3. In the absence of *M. f. fascicularis* fossil data allowing us to date interpopulational divergences, calibration of the tree is difficult. Therefore, we decided to calibrate it at node 0, which separates *M. fascicularis* and *M. mulatta* clusters. Among all the dates proposed, we chose 1.6 million years before present (My BP) as the most probable divergence time between the 2 macaque species. This divergence time was deduced from a composite estimate of primate divergence times (Purvis 1995). In that

Table 1. Summary statistics for mtDNA and nuclear genetic diversity in *Macaca fascicularis fascicularis* populations

(a) Based on HVII region sequences observed in 4 *M. f. fascicularis* populations (this study)

	Diversity parameters			Neutrality tests	
Population	N_{hap} (poly sites/indel)	$\pi \times 1000$ (±SE)	h (±SE)	D (P value)	F_s^* (P value)
Indochina (68)	27 (59/6)	17.1 (±8.7)	0.932 (±0.016)	−0.33 (0.42)	−3.14 (0.18)
Indonesia (137)	35 (88/4)	32.4 (±16)	0.926 (±0.013)	0.58 (0.21)	1.68 (0.28)
Philippines (25)	6 (16/0)	8.85 (±4.93)	0.693 (±0.082)	0.82 (0.18)	3.66 (0.07)
Mauritius (74)	2 (1/0)	0.046 (±0.164)	0.027 (±0.026)	−1.06 (0.11)	−1.97 (0.04)

(b) Based on HVI region sequences observed in 4 *M. f. fascicularis* populations (Smith et al. 2007)

	Diversity parameters			Neutrality tests	
Population	N_{hap} (poly sites)	$\pi \times 1000$ (±SE)	h (±SE)	D (P value)	F_s^* (P value)
Indochina (89)	48 (107)	83.9 (±41.4)	0.975 (±0.0064)	−0.04 (0.57)	−6.29 (0.12)
Indonesia (70)	58 (179)	183.7 (±89.3)	0.994 (±0.0035)	0.80 (0.16)	−10.39 (0.03)
Philippines (83)	34 (124)	59.5 (±29.8)	0.78 (±0.05)	−1.36 (0.067)	−2.23 (0.31)
Mauritius (68)	9 (15)	2.9 (±2.4)	0.298 (±0.073)	−2.24 (0.001)	−5.21 (0.005)

(c) Based on the microsatellite dataset from Bonhomme et al. (2007)

	Diversity parameters		Diversity parameters	
	MHC		non-MHC	
Population	n_A	H_e	n_A	H_e
Indochina (70)	12	0.80	12	0.81
Java (38)	11	0.76	9	0.83
Philippines (65)	8	0.68	8	0.74
Mauritius (81)	8	0.70	7	0.69

The number of individuals studied follows the population name; N_{hap} = Numbers of haplotypes in each population; poly sites = number of polymorphic sites; indel: number of insertion–deletions in each population sample; π = mean number of pairwise differences; SE = standard error for the sampling process; h = gene diversity; D = Tajima's D; F_S = Fu's F_S; n_A = mean number of alleles; and H_e = mean expected heterozygosity.

* Fu's F_S should be considered as significant at the 5% level if $P < 0.02$. NB: MHC and non-MHC datasets each consists of 7 microsatellite markers.

study, the baboon–macaque divergence time was proposed at around 9.25 My BP (mean value), a date compatible with more recent estimates (Raaum et al. 2005; Steiper and Young 2006). Moreover, the 1.6 My estimate for *M. mulatta* and *M. fascicularis* divergence time is in the range of dates proposed by Hayasaka et al. (1996) for the radiation of Asian macaques. With node 0 of Figure 3 being calibrated at 1.6 My BP, nodes 1, 2, and 3 become 1.2, 0.55, and 0.11 My BP, respectively. The divergence observed at node 1 corresponds to the separation between groups I and II, namely between the continental and insular groups of *M. f. fascicularis*, whereas nodes 2 and 3 correspond to the divergence time of Indochinese and Philippines populations, respectively.

Discussion

Monophyly of *Macaca fascicularis fascicularis*

This study, based on 4 *M. f. fascicularis* populations, clearly confirms that this subspecies is supported as a monophyletic mtDNA lineage by reference to other macaques (*M. mulatta*, *M. fuscata*, and *M. sylvanus*). This is in accordance with the mtDNA phylogenies of macaque species in Tosi et al. (2002, 2003) and Smith et al. (2007). In contrast to mtDNA, the paraphyly of sequences from the Y chromosome and autosomal genes led to suspect a possible male introgression from *M. mulatta* to *M. fascicularis* in Indochina (Tosi et al. 2002, 2003). *Macaca nemestrina* is also distributed in

→

Figure 2. Bayesian phylogenetic tree of mitochondrial sequences of *Macaca fascicularis fascicularis*, with branch length. The sequence names begin by letters corresponding to the 4 populations (InCH = Indochina; InNE = Indonesian; Mau = Mauritius; and Phi = Philippines), followed by a code number identifying the sequence. When there is no number in brackets the sequence was observed in only one animal. Numbers at nodes of the tree correspond to posterior confidence values. Sequences from other macaque species (*Macaca sylvanus*, *Macaca mulatta*, and *Macaca fuscata*) are included in the tree, rooted with a baboon (*Papio hamadryas*) sequence (the DDBJ/EMBL/GenBank accession number Y18001) as outgroup. The 2 *M. fuscata* sequences in this tree were from Hayasaka et al. (1991), and all other sequences were newly determined in this study.

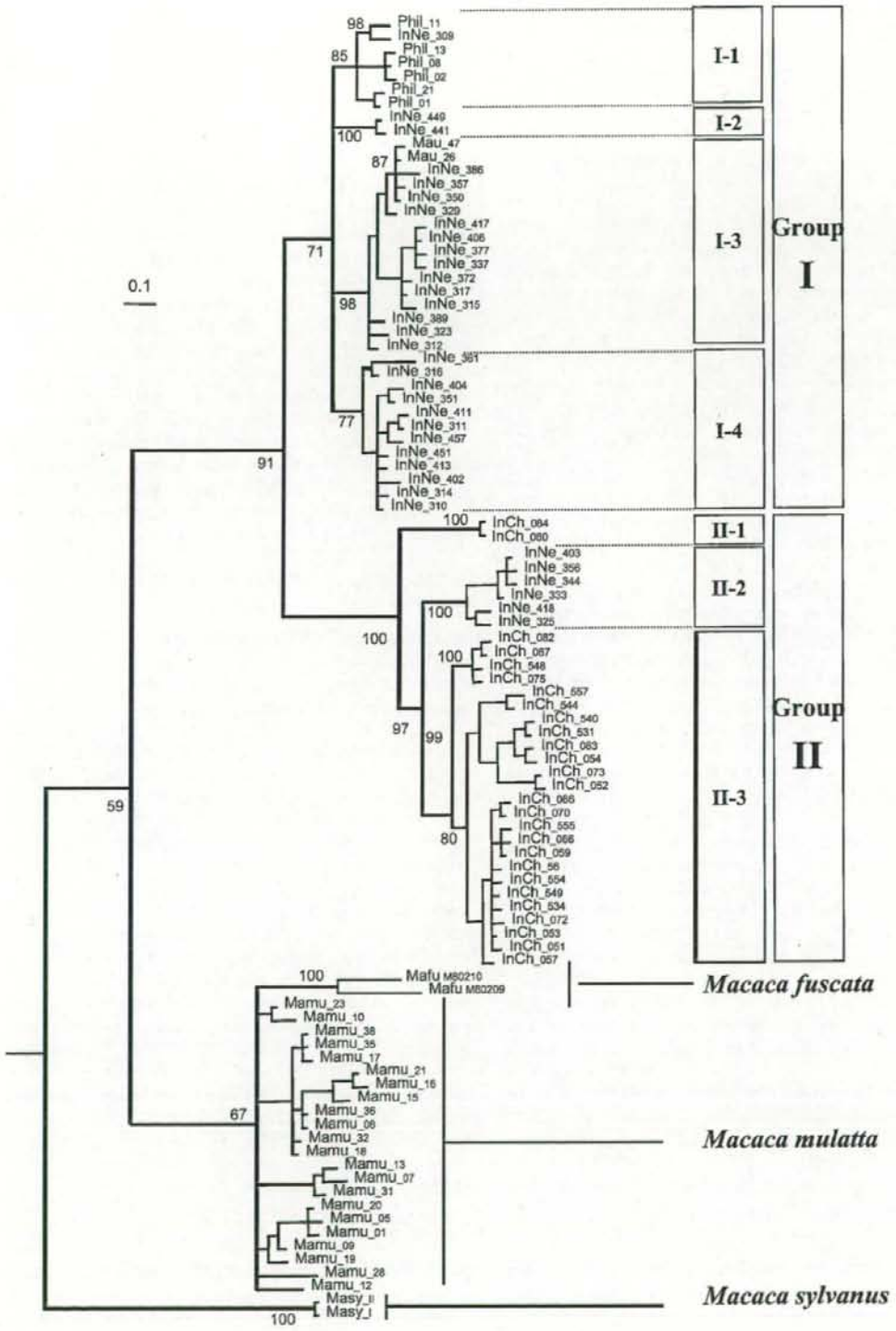
0.1
Phil_11
InNe_309
Phil_13
Phil_08
Phil_02
Phil_21
Phil_01
InNe_449
InNe_441
Mau_47
Mau_26
InNe_386
InNe_357
InNe_350
InNe_329
InNe_417
InNe_406
InNe_377
InNe_337
InNe_372
InNe_317
InNe_315
InNe_389
InNe_323
InNe_312
InNe_361
InNe_316
InNe_404
InNe_351
InNe_411
InNe_311
InNe_457
InNe_451
InNe_413
InNe_402
InNe_314
InNe_310
InCh_084
InCh_080
InNe_403
InNe_356
InNe_344
InNe_333
InNe_418
InNe_325
InCh_082
InCh_067
InCh_548
InCh_075
InCh_557
InCh_544
InCh_540
InCh_531
InCh_083
InCh_054
InCh_073
InCh_052
InCh_066
InCh_070
InCh_555
InCh_066
InCh_059
InCh_56
InCh_554
InCh_549
InCh_534
InCh_072
InCh_053
InCh_051
InCh_057
Mafu M80210
Mafu M80209
Mamu_23
Mamu_10
Mamu_38
Mamu_35
Mamu_17
Mamu_21
Mamu_16
Mamu_15
Mamu_36
Mamu_06
Mamu_32
Mamu_18
Mamu_13
Mamu_07
Mamu_31
Mamu_20
Mamu_05
Mamu_01
Mamu_09
Mamu_19
Mamu_28
Mamu_12
Masy_II
Masy_I
I-1
I-2
I-3
I-4
Group I
II-1
II-2
II-3
Group II
Macaca fuscata
Macaca mulatta
Macaca sylvanus

Indonesia, as well as *M. fascicularis* and this could again be a possible source of introgression. Therefore, when inferring the phylogenetic relationships of macaque species, caution should be taken as for the choice of the molecular markers and for the sampling of species and populations.

Origin and Genetic Diversity of the Mauritius Macaque Population

Among the 4 populations studied here, that from Mauritius clearly shows distinct polymorphism patterns. We found that most animals (73 out of 74) have the same sequence, whereas the remaining animal differs by only one nucleotide position. The latter sequence was validated twice by sequencing the DNA obtained from 2 independent PCRs. In 6 animals of the Indonesian sample, we found sequences strictly identical to the most frequent Mauritius haplotype, confirming that Indonesia is a very probable source of the Mauritius population founders. This result is compatible with the Javanese origin previously suggested by different studies (Sussman and Tattersall 1981; Kondo et al. 1993; Kawamoto Y, Kawamoto S, et al. 2008). However, recently, Tosi and Coke (2007) clearly demonstrated a mixed origin of the Mauritius population, with a Javanese or Sumatran maternal lineage, and a continental Y chromosome lineage currently found in Sumatra. In the same way, recent results obtained on DRB exon 2 polymorphism show that the Mauritius population shares several DRB sequences with not only Indonesian but also Indochinese cynomolgus macaques (9 and 6 sequences, respectively), and only 2 sequences with the Philippines (Blancher et al. 2006, and additional unpublished data from A. Blancher). Thus, the study of Tosi and Coke (2007) and our observations lead to propose the mixed origin of the Mauritius population as the most probable hypothesis.

Most probably, the low-frequency Mauritius haplotype (1%), not observed in the Indonesian sample, may have arisen by mutation (T → C) from the main haplotype, after *M. f. fascicularis* became established in Mauritius 300–500 years ago. These results are in agreement with the study of Kawamoto Y, Kawamoto S, et al. (2008) who described 2 haplotypes (S and L) of an HVII fragment sequenced on the same number of individuals, with the low-frequency haplotype at 9%. The extremely low nucleotide and genetic diversities found in the Mauritius sample is most probably the current molecular signature of a founding effect, with few females, that was firstly deduced by Lawler et al. (1995) using RFLP. Our results, which clearly demonstrate that the Mauritius population is much less polymorphic ($h = 0.03$) than the Philippines one ($h = 0.69$) for mtDNA, differ from those recently observed for DRB exon 2 polymorphism in these 2 insular populations (Blancher et al. 2006). From this DRB dataset, the expected heterozygosity values were similar between the Mauritius ($h = 0.78$) and Philippines samples ($h = 0.81$). In addition, genetic data from other studies of the nuclear genome emphasize the discrepancy observed between mtDNA and nuclear genomes in Mauritius: Average H_e from microsatellite data equaled 0.66 (Kawamoto Y, Kawamoto S, et al. 2008), 0.70, and 0.69 for MHC and non-MHC microsatellite data (Table 1c, Bonhomme et al. 2007). This discrepancy between mtDNA and nuclear (microsatellite and DRB) markers in Mauritius could have several levels of explanation: 1) the effective size (N_e) of the mtDNA is 1/4 the nuclear genes, so the probability for the Mauritius population to retain and/or maintain polymorphism after a recent founding event (~100 generations) is much lower for mtDNA than for nuclear genes; 2) the approximate date of the Philippines foundation is very much older than that of Mauritius (0.11 My BP instead of 400 years BP) and after such a long period following the colonization, mtDNA polymorphism in the Philippines population had enough time to be restored; and 3) a biased sex ratio toward males in the Mauritius founders may explain the rapid loss of mtDNA lineages. Under this hypothesis, the male founders (continental/Sumatran origin, Tosi and Coke 2007) could have strongly contributed to Mauritius cynomolgus macaque nuclear polymorphism.

Dispersal Scenario of *Macaca fascicularis fascicularis* Populations

Based on the mtDNA sequence analysis of 3 natural *M. f. fascicularis* populations, we propose the following dispersal scenario (see Figure 4). First, the ancestral population of *M. f. fascicularis* diverged (see also Harihara et al. 1988) into 2 subpopulations: one called continental, colonizing the Indochinese peninsula and the other, called insular, almost 1 My BP. This estimate is close to that proposed by Tosi et al. (2003; see also Tosi and Coke 2007).

A more precise past history of the cynomolgus macaque is given by the phylogenetic tree: 6 Indonesian haplotypes (group II-2 of Figure 2) cluster in the continental group of sequences (group II of Figure 2). This suggests the current presence in Indonesia of mtDNA lineages coming directly from the Indochinese peninsula via migrant individuals. Alternatively, those lineages may originate from a remnant population that was localized in the Sunda Shelf and closely connected to the Indochinese peninsula, during the complex dynamics of sea level change in this region at Pleistocene glacial periods (<550,000 years BP). Figure 4 shows the putative location on the Sunda Shelf of such an ancient population and gives possible migrations routes explaining the paraphyly of Indonesian haplotypes.

More recently, around 110 000 years BP, the Philippines population derived from an Indonesian *M. f. fascicularis* stock (see Figure 3). Invasion of the Philippines may have been possible by terrestrial access through Borneo during periods of low sea level in Southeast Asia. An alternative scenario is

→

Figure 3. Bayesian phylogenetic tree of *Macaca fascicularis* populations, under the assumption of a constant mutation rate. Circles represent the nodes 0, 1, 2, and 3 that are dated at 1.6, 1.2, 0.55, and 0.11 My, respectively.

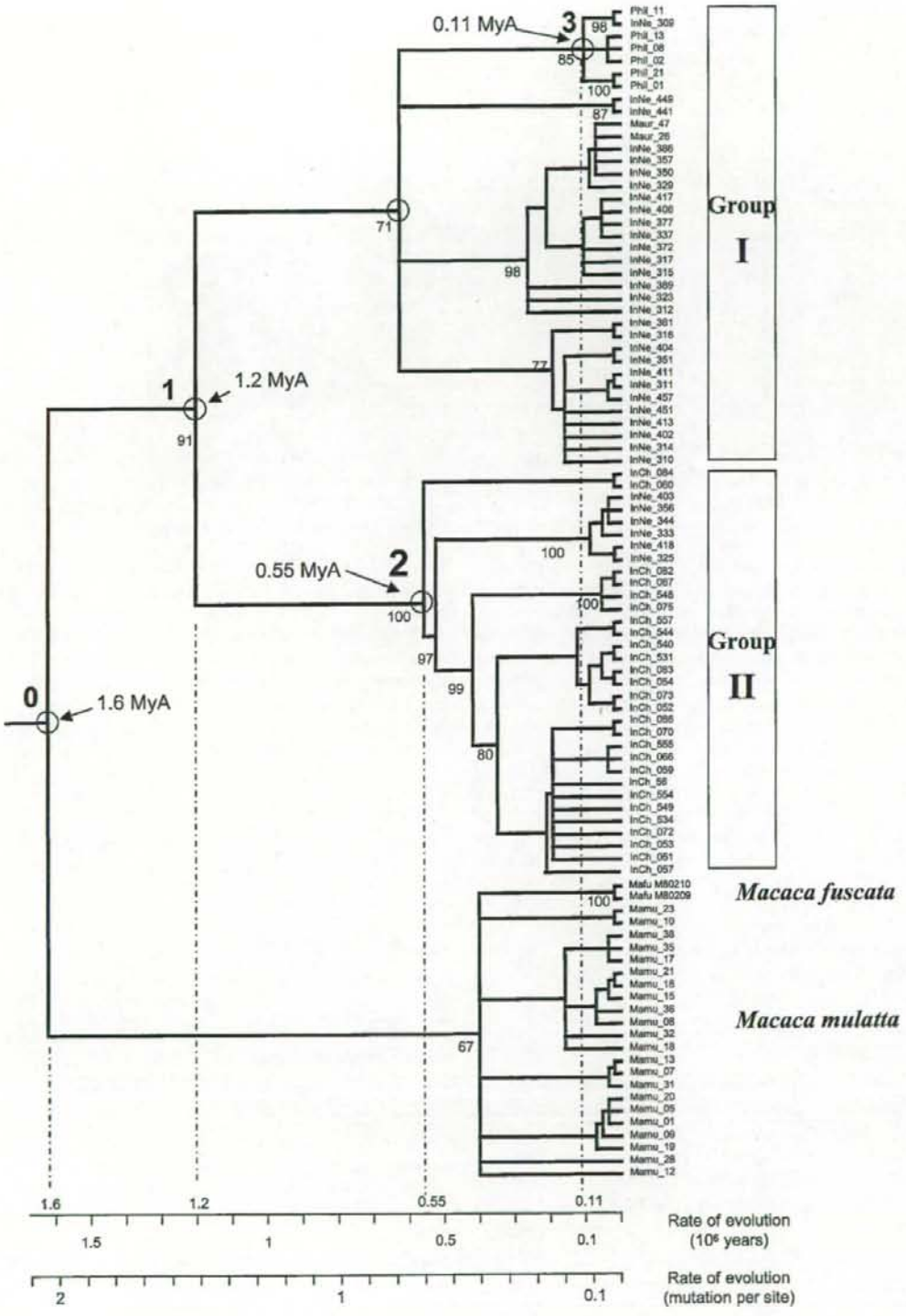
0.11 MyA
3
1.2 MyA
1
0.55 MyA
2
1.6 MyA
0
Group I
Group II
Macaca fuscata
Macaca mulatta
Rate of evolution (10⁶ years)
Rate of evolution (mutation per site)

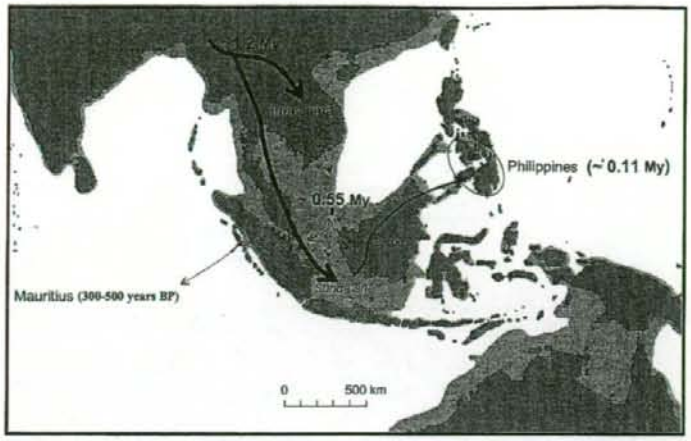

Figure 4. Map depicting the dispersal of *Macaca fascicularis fascicularis* in Southeast Asia. The figure was adapted from the original map from Voris (2000) where the limits of −120 m below present sea level are shown in light gray. Solid arrows depict the initial split between continental and insular groups and the colonization event of the Philippines. Dashed arrows depict hypothetic dispersal subsequent to the initial split. Dotted arrows represent the putative origins of the Mauritius population.

that, given that *M. fascularis* live in mangroves near the coast, it could have colonized the Philippines from Indonesia via Borneo by sea rafting (Abegg and Thierry 2002).

Most probably, all current Philippines haplotypes reported here have derived from a single common ancestral haplotype. The low genetic and nucleotide diversities suggest that a small group of Indonesian animals colonized the Philippines. Although precise dating of Philippines colonization cannot be assessed from our results, the phylogenetic tree suggests that after colonization of the Philippines, the population essentially remained isolated from the Indonesian population, allowing divergence of Philippines haplotypes that are not observed in the Indonesian sample. Although most Philippines sequences cluster in a specific group, this group encompasses one sequence from Indonesia. The latter could derive from the same ancestral haplotype, which gave rise to the Philippines population, but we cannot exclude back migration from the Philippines to Indonesia (Harihara et al. 1988).

Conclusions

The analysis of mtDNA D-loop sequences and further observations of nuclear genetic data confirms the founding of the Mauritius population by a small number of animals imported from Indonesia and perhaps also Indochina, as previously suggested by Tosi and Coke (2007). Our results also support the previously suggested ancient differentiation of *M. f. fascicularis* into 2 subgroups: 1 continental, another insular. In addition, our data raise the complexity of the Indonesian population. Indeed, the similarity between some sequences from Indonesia (subgroup II-2) and Indochina suggests either subsequent migrations southward, from Indochina to Indonesia, or an early colonization of the Sunda Shelf by the Indochinese population and then migrations southward, to Indonesia. The Philippines were most probably colonized by a small number of Indonesian *M. f. fascicularis* individuals. Unfortunately, the paucity of *M. f. fascicularis* fossil data in South East Asia and the uncertainty in calibrating the phylogenetic tree make divergence times dating difficult to assess in the light of complex and periodic changes in paleoclimates in Southeast Asia.

Funding

French Ministry of Research grant (contract EA3034 to A.B); Japanese Ministry of Education, Sport, Science, and Technology (to N.S.).

Acknowledgments

We thank, for their excellent technical assistance, Stéphanie Despiau, Béatrice Atlan, and Yoshimi Noaki. We also thank Dr. Jeffry Rogers for informing us of the paper of Smith et al. before publication and Dr. David Glenn Smith for sending us the geographical origins of all the cynomolgus macaque individuals they studied.

References

Abegg C, Thierry B. 2002. Macaque evolution and dispersal in insular south-east Asia. Biol J Linn Soc. 75:555–576.

Bensasson D, Zhang D, Hartl DL, Hewitt GM. 2001. Mitochondrial pseudogenes: evolution's misplaced witnesses. Trends Ecol Evol. 16:314–321.

Blancher A, Tisseyre P, Dutaur M, Apoil PA, Maurer C, Quesniaux V, Raulf F, Bigaud M, Abbal M. 2006. Study of Cynomolgus monkey (*Macaca fascicularis*) MhcDRB (Mafa-DRB) polymorphism in two populations. Immunogenetics. 58:269–282.

Bonhomme M, Blancher A, Jalil FM, Crouau-Roy B. 2007. Factors shaping genetic variation in the MHC of natural non-human primate populations. Tissue Antigens. 70:398–411.

Borie D, Hausen B, Larson M, Klupp J, Stalder M, Birsan T, Morris R. 2002. A life-supporting technique of renal allotransplantation in *Macaca fascicularis* to evaluate novel immunosuppressive drugs in nonhuman primates. J Surg Res. 107:64–74.

Delson E. 1980. Fossil macaques, phyletic relationships and a scenario of deployment. In: Lindburg DG, editor. The macaques: studies in ecology, behavior and evolution, New York: Van Nostrand Reinhold Company. p. 10–30.

Eudey A. 1980. Pleistocene glacial phenomena and the evolution of Asian macaques. In: Lindburg DG, editor. The macaques: studies in ecology, behavior and evolution, New York: Van Nostrand Reinhold Company. p. 52–83.

Fittinghoff NA, Lindburg DG. 1980. Riverine refuging in east bornean *Macaca fascicularis*. In: Lindburg DG, editor. The macaques: studies in ecology, behavior and evolution, New York: Van Nostrand Reinhold Company. p. 215–245.

Fooden J. 1991. Systematic review of Philippine macaques (primates, cercopithecidae: *Macaca fascicularis* subspp). Field Zool. 64:1–44.

Fooden J. 1995. Systematic review of Southeast Asian longtail macaques, *Macaca fascicularis* [Raffles, (1821)]. Field Zool. 81:1–206.

Fu YX. 1997. Statistical tests of neutrality against population growth, hitchhiking and background selection. Genetics. 147:915–925.

Guindon S, Gascuel O. 2003. A simple, fast, and accurate algorithm to estimate large phylogenies by maximum-likelihood. Syst Biol. 52:696–704.

Harihara S, Saitou N, Hirai M, Aoto N, Terao K, Cho F, Honjo S, Omoto K. 1988. Differentiation of mitochondrial DNA types in *Macaca fascicularis*. Primates. 29:117–127.

Hayasaka K, Fujii K, Horai S. 1996. Molecular phylogeny of macaques: implications of nucleotide sequences from an 896-base pair region of mitochondrial DNA. Mol Biol Evol. 13:1044–1053.

Hayasaka K, Ishida T, Horai S. 1991. Heteroplasmy and polymorphism in the major noncoding region of mitochondrial DNA in Japanese monkeys: association with tandemly repeated sequences. Mol Biol Evol. 8:399–415.

Kawamoto Y, Kawamoto S, Matsubayashi K, Nozawa K, Watanabe T, Stanley M-A, Perwitasari-Farajallah D. 2008. Genetic diversity of longtail macaques (*Macaca fascicularis*) on the island of Mauritius: an assessment of nuclear and mitochondrial DNA polymorphisms. J Med Primatol. 37:45–54.

Kawamoto Y, Shotake T, Nozawa K, Kawamoto S, Tomari K, Mawai S, Shiri K, Morimitsu Y, Takagi N, Akaza H, et al. 2007. Postglacial population expansion of Japanese macaques (*Macaca fuscata*) inferred from mitochondrial DNA phylogeography. Primates. 48:27–40.

Kimura M. 1980. A simple method for estimating evolutionary rates of base substitutions through comparative studies of nucleotide sequences. J Mol Evol. 16:111–120.

Kita Y, Tanaka T, Yoshida S, Ohara N, Kaneda Y, Kuwayama S, Muraki Y, Kanamaru N, Hashimoto S, Takai H, et al. 2005. Novel recombinant BCG and DNA-vaccination against tuberculosis in a cynomolgus monkey model. Vaccine. 23:2132–2135.

Kondo M, Kawamoto Y, Nozawa K, Matsubayashi K, Watanabe T, Griffiths O, Stanley MA. 1993. Population genetics of crab-eating macaques (*Macaca fascicularis*) on the island of Mauritius. Am J Primatol. 29:167–182.

Kuiken T, Rimmelzwaan GF, Van Amerongen G, Osterhaus AD. 2003. Pathology of human influenza A (H5N1) virus infection in cynomolgus macaques (*Macaca fascicularis*). Vet Pathol. 40:304–310.

Kumar S, Tamura K, Nei M. 2004. MEGA3: integrated software for molecular evolutionary genetics analysis and sequence alignment. Brief Bioinform. 5:150–163.

Lau M, Vayntrub T, Grumet FC, Lowsky R, Strober S, Hoppe R, Larson M, Holm B, Reitz B, Borie D. 2004. Short tandem repeat analysis to monitor chimerism in *Macaca fascicularis*. Am J Transplant. 4:1543–1548.

Lawler JV, Endy TP, Hensley LE, Garrison A, Fritz EA, Lesar M, Baric RS, Kulesh DA, Norwood DA, Wasieloski LP, et al. 2006. Cynomolgus macaque as an animal model for severe acute respiratory syndrome. PLoS Med. 3:e149.

Lawler SH, Sussman RW, Taylor LL. 1995. Mitochondrial DNA of the Mauritian macaques (*Macaca fascicularis*): an example of the founder effect. Am J Phys Anthropol. 96:133–141.

Marmi J, Bertranpetit J, Terradas J, Takenaka O, Domingo-Roura X. 2004. Radiation and phylogeography in the Japanese macaque, *Macaca fuscata*. Mol Phylogenet Evol. 30:676–685.

Melnick DJ, Hoelzer GA. 1992. Differences in male and female macaque dispersal lead to contrasting distributions of nuclear and mitochondrial DNA variation. Int J Primatol. 13:379–393.

Menninger K, Wieczorek G, Riesen S, Kunkler A, Audet M, Blancher A, Schuurman HJ, Quesniaux V, Bigaud M. 2002. The origin of cynomolgus monkey affects the outcome of kidney allografts under Neoral immunosuppression. Transplant Proc. 34:2887–2888.

Meyer S, Weiss G, von Haeseler A. 1999. Pattern of nucleotide substitution and rate heterogeneity in the hypervariable regions I and II of human mtDNA. Genetics. 152:1103–1110.

Modolo L, Salzburger W, Martin RD. 2005. Phylogeography of barbary macaque (*Macaca sylvanus*) and the origin of the Gibraltar colony. Proc Natl Acad Sci USA. 102:7392–7397.

Nei M. 1987. Molecular evolutionary genetics. New York: Columbia University Press.

Nozawa K, Shotake T, Ohkura Y, Tanabe Y. 1977. Genetic variations within and between species of Asian macaques. Jpn J Genet. 52:15–30.

Posada D, Crandall KA. 1998. MODELTEST: testing the model of DNA substitution. Bioinformatics. 14:817–818.

Purvis A. 1995. A composite estimate of primate phylogeny. Philos Trans R Soc Lond B Biol Sci. 348:405–421.

Raaum RL, Sterner KN, Noviello CM, Stewart CB, Disotell TR. 2005. Catarrhine primate divergence dates estimated from complete mitochondrial genomes: concordance with fossil and nuclear DNA evidence. J Hum Evol. 48:237–257.

Reed DS, Larsen T, Sullivan LJ, Lind CM, Lackemeyer MG, Pratt WD, Parker MD. 2005. Aerosol exposure to western equine encephalitis virus causes fever and encephalitis in cynomolgus macaques. J Infect Dis. 192: 1173–1182.

Ronquist F, Huelsenbeck JP. 2003. MrBayes 3: Bayesian phylogenetic inference under mixed models. Bioinformatics. 19:1572–1574.

Saitou N, Nei M. 1987. The neighbor-joining method: a new method for reconstructing phylogenetic trees. Mol Biol Evol. 4:406–425.

Sato H, Kobune F, Ami Y, Yoneda M, Kai C. 2008. Immune responses against measles virus in cynomolgus monkeys. Comp Immunol Microbiol Infect Dis. 31:25–35.

Schmidt LH, Fradkin R, Harrison J, Rossan RN. 1977. Differences in the virulence of Plasmodium knowlesi for *Macaca irus* (*fascicularis*) of Philippine and Malayan origins. Am J Trop Med Hyg. 26(4):612–622.

Schneider S, Roessli D, Excoffier L. 2000. Arlequin ver. 2000: a software for population genetics data analysis. Geneva (Switzerland): Genetics and Biometry Laboratory, University of Geneva.

Schroder C, Pierson RN 3rd, Nguyen BN, Kawka DW, Peterson LB, Wu G, Zhang T, Springer MS, Siciliano SJ, Iliff S, et al. 2007. CCR5 blockade modulates inflammation and alloimmunity in primates. J Immunol. 179: 2289–2299.

Smith DG, McDonough J. 2005. Mitochondrial DNA variation in Chinese and Indian rhesus macaques (*Macaca mulatta*). Am J Primatol. 65:1–25.

Smith DG, McDonough JW, George DA. 2007. Mitochondrial DNA variation within and among regional populations of longtail macaques (*Macaca fascicularis*) in relation to other species of the fascicularis group of macaques. Am J Primatol. 69:182–198.

Steiper ME, Young NM. 2006. Primate molecular divergence dates. Mol Phylogenet Evol. 41:384–394.

Sussman RW, Tattersall I. 1981. Behavior and ecology of *Macaca fascicularis* in Mauritius: a preliminary study. Primates. 22:192–205.

Sussman RW, Tattersall I. 1986. Distribution, abundance, and putative ecological strategy of *Macaca fascicularis* on the island of Mauritius, southwestern Indian Ocean. Folia Primatol. 46:28–43.

Tajima F. 1989. Statistical method for testing the neutral mutation hypothesis by DNA polymorphism. Genetics. 123:585–595.

Terao K, Fujimoto K, Cho F, Honjo S. 1981. Inheritance and distribution of human-type A-B-O blood groups in cynomolgus monkeys. J Med Primatol. 10:72–80.

Thalmann O, Hebler J, Poinar HN, Paabo S, Vigilant L. 2004. Unreliable mtDNA data due to nuclear insertions: a cautionary tale from analysis of humans and other great apes. Mol Ecol. 13:321–335.

Thalmann O, Serre D, Hofreiter M, Lukas D, Eriksson J, Vigilant L. 2005. Nuclear insertions help and hinder inference of the evolutionary history of gorilla mtDNA. Mol Ecol. 14:179–188.

Tosi AJ, Coke CS. 2007. Comparative phylogenetics offer new insights into the biogeographic history of *Macaca fascicularis* and the origin of the Mauritian macaques. Mol Phyl Evol. 42:498–504.

Tosi AJ, Morales JC, Melnick DJ. 2002. Y-chromosome and mitochondrial markers in *Macaca fascicularis* indicate introgression with Indochinese *M. mulatta* and a biogeographic barrier in the Isthmus of Kra. Int J Primatol. 23:161–178.

Tosi AJ, Morales JC, Melnick DJ. 2003. Paternal, maternal, and biparental molecular markers provide unique windows onto the evolutionary history of macaque monkeys. Evolution. 57:1419–1435.

Voris HK. 2000. Maps of Pleistocene sea levels in Southeast Asia: shorelines, river systems and time durations. J Biogeogr. 27:1153–1167.

Wheatley BP. 1980. Feeding and ranging of East Bornean *Macaca fascicularis*. In: Lindburg DG, editor. The macaques: studies in ecology, behavior and evolution, New York: Van Nostrand Reinhold Company. p. 215–245.

Wieczorek G, Bigaud M, Menninger K, Riesen S, Quesniaux V, Schuurman HJ, Audet M, Blancher A, Mihatsch MJ, Nickeleit V. 2006. Acute and chronic vascular rejection in nonhuman primate kidney transplantation. Am J Transplant. 6:1285–1296.

Received April 19, 2007
Accepted November 27, 2007

Corresponding Editor: Jill Pecon-Slattery

blood

2008 111: 243-250
Prepublished online Sep 24, 2007;
doi:10.1182/blood-2007-04-086017

Interaction between Hck and HIV-1 Nef negatively regulates cell surface expression of M-CSF receptor

Masateru Hiyoshi, Shinya Suzu, Yuka Yoshidomi, Ranya Hassan, Hideki Harada, Naomi Sakashita, Hirofumi Akari, Kazuo Motoyoshi and Seiji Okada

Blood (print ISSN 0006-4971, online ISSN 1528-0020), is published semimonthly by the American Society of Hematology, 1900 M St, NW, Suite 200, Washington DC 20036.

Interaction between Hck and HIV-1 Nef negatively regulates cell surface expression of M-CSF receptor

Masateru Hiyoshi,[1] Shinya Suzu,[1] Yuka Yoshidomi,[1] Ranya Hassan,[1] Hideki Harada,[1] Naomi Sakashita,[2] Hirofumi Akari,[3] Kazuo Motoyoshi,[4] and Seiji Okada[1]

[1]Division of Hematopoiesis, Center for AIDS Research; [2]Department of Cell Pathology, Graduate School of Medical and Pharmaceutical Sciences, Kumamoto University, Kumamoto; [3]Laboratory of Disease Control, Tsukuba Primate Research Center, National Institute of Biomedical Innovation, Ibaraki; and [4]Third Department of Internal Medicine, National Defense Medical College, Saitama, Japan

Nef is a multifunctional pathogenetic protein of HIV-1, the interaction of which with Hck, a Src tyrosine kinase highly expressed in macrophages, has been shown to be responsible for the development of AIDS. However, how the Nef-Hck interaction leads to the functional aberration of macrophages is poorly understood. We recently showed that Nef markedly inhibited the activity of macrophage colony-stimulating factor (M-CSF), a primary cytokine for macrophages. Here, we show that the inhibitory effect of Nef is due to the Hck-dependent down-regulation of the cell surface expression of M-CSF receptor Fms. In the presence of Hck, Nef induced the accumulation of an immature under–N-glycosylated Fms at the Golgi, thereby down-regulating Fms. The activation of Hck by the direct interaction with Nef was indispensable for the down-regulation. Unexpectedly, the accumulation of the active Hck at the Golgi where Nef prelocalized was likely to be another critical determinant of the function of Nef, because the expression of the constitutive-active forms of Hck alone did not fully down-regulate Fms. These results suggest that Nef perturbs the intracellular maturation and the trafficking of nascent Fms, through a unique mechanism that required both the activation of Hck and the aberrant spatial regulation of the active Hck. (Blood. 2008;111:243-250)

Introduction

HIV-1 infections lead to the development of AIDS by causing progressive degeneration of the immune system.[1-3] The main cellular targets of HIV-1 are CD4$^+$ T cells and macrophages, and the depletion of CD4$^+$ T cells caused by an infection is suggested to account for many aspects of the pathogenesis of HIV-1.[1-3] Meanwhile, a number of studies have revealed the functional aberration of HIV-1–infected macrophages.[4,5] Infected macrophages showed an altered profile of the production of cytokine/chemokines[4] or migratory capacity,[5] which might contribute to the uncontrolled homeostasis of the immune system. Indeed, functional analyses of HIV-1 Nef protein have revealed that macrophages as well as CD4$^+$ T cells play an important role in the development of AIDS.

Nef is a 25- to 30-kDa protein with no enzymatic activity encoded by the HIV-1 genome.[6,7] Studies of HIV-1–infected patients have clearly demonstrated Nef to be a critical determinant of the development of AIDS: HIV-1 strains without an intact Nef gene were frequently isolated from nonprogressive long-term survivors.[8,9] Subsequent study of HIV-1 transgenic mice confirmed the pathogenetic activity of Nef: targeted expression of the entire coding sequence of HIV-1 in CD4$^+$ T cells and macrophages caused a severe AIDS-like disease in mice, which was completely abolished by the disruption of the Nef gene.[10] Importantly, only an amino acid substitution in the proline-rich (PxxP) motifs of Nef was sufficient to protect mice from the development of AIDS-like disease.[11] A number of studies have revealed that Nef interacts with a subset of cellular Src family tyrosine kinases, via the PxxP motifs.[12-15] The Nef PxxP motifs had an affinity for the Src homology (SH3) domain of Hck, Lyn, and possibly c-Src, but not of Fgr, Fyn, Lck, and Yes.[12-15] In particular, the interaction between the Nef PxxP motifs and the Hck SH3 domain was likely to be important, because the interaction caused the activation of Hck.[13-15] Indeed, a study with HIV-1 transgenic mice clearly demonstrated the importance of the Nef-Hck interaction for the development of AIDS: the appearance of the AIDS-like disease was significantly delayed when the HIV-1 transgenic mice expressing an intact Nef gene were crossed with an *hck*$^{-/-}$ background.[11] Given that Hck is expressed in macrophages but not in CD4$^+$ T cells,[16] the finding indicates that the Nef-Hck interaction in macrophages is at least in part responsible for the development of AIDS. However, little is known of the molecular mechanisms by which the Nef-Hck interaction contributes to the functional aberration of macrophages and the development of AIDS. The fact that Src kinases including Hck have both positive and negative roles in cell signaling pathways[16-19] makes it difficult to predict the functional consequences of the Nef-Hck interaction.

A well-characterized function of Nef is the down-regulation of the cell surface expression of CD4[6,7,20] or major histocompatibility complex class I (MHC I).[6,7,21-23] Nef accelerates the endocytosis of CD4,[20] the receptor for HIV-1,[1-3] which allows an efficient viral release from the host cells.[6,7] Nef reduces the level of the surface expression of MHC I through multiple mechanisms,[21-23] which diminishes the recognition of the infected cells by cytotoxic T cells.[6,7] However, these hallmark functions of Nef may not fully account for the functional significance of the Nef-Hck interaction,

Submitted April 17, 2007; accepted September 18, 2007. Prepublished online as *Blood* First Edition paper, September 24, 2007; DOI 10.1182/blood-2007-04-086017.

The online version of this article contains a data supplement.

The publication costs of this article were defrayed in part by page charge payment. Therefore, and solely to indicate this fact, this article is hereby marked "advertisement" in accordance with 18 USC section 1734.

because the down-regulation of CD4 or MHC I occurs even in the absence of Hck (ie, in $CD4^+$ T cells).[20-23] Meanwhile, we and others have recently identified the functions of Nef that are dependent on Hck.[24-26] Drakesmith et al demonstrated that Nef down-regulated the surface expression of HFE, an iron homeostasis regulator expressed on macrophages, which was abolished by a dominant-negative Hck.[24] Briggs et al demonstrated that Nef mimicked the cell growth–promoting activity of granulocyte-macrophage colony-stimulating factor (GM-CSF), a cytokine that supports the proliferation and differentiation of monocyte/macrophages,[27] possibly through a mechanism that required Hck and the Stat3 transcription factor.[25] Nef might contribute to the survival of macrophages by mimicking GM-CSF receptor pathways, allowing long-term viral replication.[25] In contrast to the latter finding, we demonstrated that Nef inhibited the growth of human myeloid leukemia TF-1-fms cells mediated by macrophage colony-stimulating factor (M-CSF),[26] another cytokine essential for the proliferation and differentiation of monocytes/macrophages.[28] The growth inhibition of the cells correlated well with the impaired activation of the M-CSF receptor Fms,[26] which is a tyrosine kinase encoded by the proto-oncogene *c-fms*.[28] Impaired activation of Fms was also observed in human embryonic 293 cells coexpressing Nef and Hck, but not in cells expressing Nef alone or Hck alone.[26] Thus, these data indicated that Nef inhibited the activation of Fms through a mechanism that required Hck.

The functions of macrophages are distinctly regulated by M-CSF and GM-CSF,[27,28] as evidenced by the marked difference in the morphology of macrophages derived from these cytokines.[29] Moreover, these macrophages showed different profiles of the production of chemokines/cytokines.[29] Thus, it is possible that Nef affects the functions of macrophages by differently modulating the activities of M-CSF and GM-CSF, contributing to the uncontrolled immune system. However, little is known of the molecular mechanisms by which Nef differently modulates the activities of these cytokines, through the common target Hck. In this study, we therefore attempted to clarify how the Nef-Hck interaction caused the impaired activation of Fms.

Methods

Hematopoietic cell lines and culture conditions

Human myeloid leukemia TF-1 cells[30] were maintained with RPMI1640 medium supplemented with 10% FCS and 2 ng/mL recombinant human GM-CSF (rhGM-CSF; PeproTech, Rocky Hill, NJ). TF-1-fms cells,[31] which were obtained by introducing the plasmid pCEF-c-fms encoding the human *c-fms* gene into the TF-1 cells, were maintained with RPMI1640–10% FCS in the presence of 100 ng/mL rhM-CSF (a gift from Morinaga Milk Industry, Kanagawa, Japan) and 200 μg/mL G418 (Calbiochem, Darmstadt, Germany). TF-1-fms-Nef-ER cells[26] were obtained by introducing pEBB-Nef-ER-IRES-puro[32] into TF-1-fms cells, and maintained in the presence of rhM-CSF, G418, and 1.5 μg/mL puromycin (Sigma, St Louis, MO). The plasmid encoded the Nef-ER fusion protein composed of Nef (derived from the NL4–3 strain of HIV-1) and the hormone-binding domain of the murine estrogen receptor (ER).[32] In this system, Nef was basally inactive but it was induced to function by the estrogen analog, 4-hydroxytamoxifen (4-HT; Sigma).[32] We also established TF-1 cells expressing the Nef-ER fusion protein (TF-1-Nef-ER) by using the same plasmid. The transfection was performed with Lipofectin reagent (Invitrogen, Carlsbad, CA), according to the manufacturer's recommendations. Transfected cells were selected in media containing rhGM-CSF and puromycin, followed by limiting dilution to isolate stable clones. The expression of Nef-ER in these clones was determined by Western blotting[26] with anti-Nef rabbit antiserum obtained through the National Institutes of Health (NIH) AIDS Research and Reference Reagent Program (Division of AIDS, National Institute of Allergy and Infectious Diseases, NIH, Bethesda, MD).[33] The cell growth was determined by colorimetric assay with MTT reagent (Sigma), and the absorbance of each culture was measured at 595 nm with a microplate reader (Thermo Electron, Vantaa, Finland). The expression of Fms on TF-1-fms-Nef-ER cells and that of GM-CSF receptors on TF-1-Nef-ER cells was analyzed on a FACSCalibur using Cell Quest Software (Becton Dickinson, Mountain View, CA).[26] Anti-Fms rat monoclonal IgG (clone 12-2D6; Zymed, South San Francisco, CA) was labeled with FITC using Fluorescein Labeling Kit-NH_2 (Dojindo, Kumamoto, Japan). FITC-labeled anti–GM-CSF receptor α chain (clone 4H1) and PE-labeled anti–GM-CSF β chain (clone 1C1) were purchased from eBioscience (San Diego, CA).

Macrophages and nucleofection

Human peripheral blood samples were collected from adults donors after informed consent was obtained in accordance with the Declaration of Helsinki and based on a protocol approved by the Institutional Review Board of the Faculty of Medical and Pharmaceutical Sciences, Kumamoto University. Monocytes were enriched from peripheral blood mononuclear cells by adherence to dishes for 1 hour. Macrophages were prepared by culturing the monocytes with RPMI1640 medium supplemented with 15% FCS and 100 ng/mL rhM-CSF for 5 to 7 days. The nucleofection with the Human Macrophage Nucleofector Kit and the Nucleofector II device (Amaxa, Cologne, Germany) was performed according to the manufacturer's recommendations. In brief, 5×10^5 macrophages were nucleofected with 5 μg plasmid and then cultured with Macrophage-SFM medium (Gibco, Grand Island, NY) supplemented with 15% FCS and 10 ng/mL rhGM-CSF for 8 to 12 hours. The nucleofected macrophages were cultured with GM-CSF, because M-CSF caused the down-regulation of Fms (Figure S2B,C). To identify the Nef-expressing macrophages, we used the pRc/CMV-CD8-Nef plasmid[34] encoding Nef (derived from the SF2 strain of HIV-1) fused to the extracellular/transmembrane regions of CD8. As a control, we used the plasmid encoding only those regions of CD8 (pRc/CMV-CD8).[34] The nucleofected macrophages were detached from the culture dishes using the enzyme-free cell dissociation buffer (Gibco), and then subjected to flow cytometric analysis on a FACSCalibur. Labeled antibodies used were PE-labeled anti-Fms (clone 3-4A4; Santa Cruz Biotechnology, Santa Cruz, CA), APC-labeled anti-CD8 (clone DK25; Dako, Glostrup, Denmark), and PE-labeled anti-CD4 (clone S3.5; Caltag, Burlingame, CA).

293 cell lines, transfection, and plasmids

Human embryonic kidney 293 cells (Invitrogen) were maintained with DME medium supplemented with 10% FCS. We also used 293 cells stably expressing Fms, both Fms and Hck, or CD4. 293-Fms cells were established by transfecting pCEF-c-fms[31] followed by the enrichment of Fms^{high} cells with a JSAN cell sorter (Bay bioscience, Kobe, Japan). 293-Fms/Hck cells were established by further transfecting a human Hck expression plasmid into the 293-Fms cells. For this purpose, Hck cDNA[35] cloned in the vector pIRES2-EGFP (Clontech, Mountain View, CA) was subcloned into pIRES-bleo3 (Clontech). An Hck^{high} clone was isolated from the transfected cells by Western blotting. 293-CD4 cells were established by transfecting pEneoMOS-CD4[36] followed by the enrichment of $CD4^{high}$ cells by the sorting. These cells were maintained with media containing 200 μg/mL G418 or 200 μg/mL phleomycin D1 (Invitrogen), or both. Transient transfection experiments with these 293 cell lines were performed essentially as described previously.[26] In brief, cells grown on a 12-well tissue culture plate were transfected with a total of 1.6 μg plasmid using LipofectAMINE2000 reagent (Invitrogen).

The transient expression of Fms was achieved with pCEF-c-fms. The transient expression of Hck was mostly achieved with Hck cDNA cloned in pcDNA3.1 (Invitrogen), except for the flow cytometric analysis in which Hck cDNA cloned in pIRES2-EGFP was used (Figure 2A). Based on an earlier report,[14] we also prepared constitutive-active (YF and AxxA) and kinase-dead (KE) forms of Hck by using QuikChange II Site-Directed Mutagenesis Kits (Stratagene, La Jolla, CA). The transient expression of Nef was achieved mostly with pRc/CMV-CD8-Nef,[34] the Nef of which was

derived from the SF2 strain of HIV-1. In a selected experiment (Figure 4A), we used Nef of the NL4-3 strain, as the mutants used in the analysis were derived from the strain. WL/AA, LL/AA, and AxxA mutants were provided by A. Adachi (University of Tokushima, Tokushima, Japan) and subcloned into the vector pRc/CMV-CD8. The M20A mutant[37] was also subcloned into this vector.

Western blotting, flow cytometry, and immunofluorescence with 293 cells

The preparation of total cell lysate and Western blotting were performed essentially as described.[26,38] In a selected experiment (Figure 2C), a monolayer of transfected 293 cells was treated with trypsin or control PBS buffer for 3 minutes at room temperature immediately prior to the lysis. Total cell lysate was also subjected to a lectin pull-down assay,[39] using wheat germ agglutinin (WGA)–agarose and concanavalin A (Con A)–agarose (both from Wako, Osaka, Japan). Alternatively, total cell lysate was treated with either endo-β-*N*-acetylglucosaminidase H (Endo-H) or peptide-*N*-glycosidase F (PNGase F) (both from Roche, Mannheim, Germany), according to the manufacturer's recommendations. Primary antibodies used were as follows: anti–N-terminal portion of Fms (H-300; Santa Cruz Biotechnology), anti–C-terminal portion of Fms (C-20; Santa Cruz Biotechnology), anti-Nef rabbit antiserum,[33] anti-Hck (clone 18; Transduction Laboratories, Lexington, KY), and anti-ERK (K-23; Santa Cruz Biotechnology).

The transfected cells were detached from the culture dishes and subjected to a flow cytometric analysis with anti–Fms-PE, anti–CD4-PE, or anti–CD8-APC as above. For immunostaining, cells were directly fixed in 2% paraformaldehyde, permeabilized with ethanol, and stained with primary antibodies for 12 hours followed by labeled secondary antibodies.[40,41] The primary antibodies used were as follows: anti-Fms rat IgG (clone 3-4A4-E4; Abcam, Cambridge, MA), anti-GM130 mouse IgG (Transduction Laboratories), anti-CD8 rabbit IgG (H-160; Santa Cruz Biotechnology), and rabbit IgG specific for Hck phosphorylated at Tyr411 (Santa Cruz Biotechnology). The labeled secondary antibodies used were as follows: anti–rat IgG-AlexaFluo488, anti–mouse IgG-AlexaFluo568, and anti–rabbit IgG-AlexaFluo488 (Molecular Probes, Eugene, OR). Nuclei were stained with DAPI (Molecular Probes). The fluorescent signals were visualized with a BZ-8000 fluorescence microscope (Keyence, Osaka, Japan) equipped with Plan-Fluor ELWD 20×/0.45 objective lenses (Nikon, Tokyo, Japan). Image processing was performed using BZ-Analyzer (Keyence) and Adobe Photoshop software (Adobe Systems, San Jose, CA).

Results

Nef selectively inhibits M-CSF–dependent growth and down-regulates Fms

In this study, we initially attempted to confirm the stimulatory effect of Nef on GM-CSF reported by another group,[25] using the same system in which we found the inhibitory effect on M-CSF.[26] We previously established human myeloid TF-1-fms cells expressing a conditionally active Nef-ER fusion protein.[26,32] Although TF-1-fms was an M-CSF–dependent clone derived from GM-CSF–dependent TF-1 cells,[30,31] TF-1-fms cells lost their growth response to GM-CSF due to long-term maintenance with M-CSF.[42] Thus, we also established TF-1 clones expressing the Nef-ER fusion proteins, the level of which was comparable with that in the pre-established TF-1-fms-Nef-ER clone (Figure S1A, available on the *Blood* website; see the Supplemental Materials link at the top of the online article). The inducible activation of Nef by the estrogen analog 4-HT was verified by the down-regulation of CD4 expression (data not shown). As shown (Figure S1A,B) and consistent with the results of the other group,[25] the activation of Nef did not inhibit but enhanced the GM-CSF–dependent growth of TF-1-Nef-ER cells, albeit slightly. However, the activation of Nef markedly inhibited the M-CSF–dependent growth of TF-1-fms-Nef-ER cells (Figure S1A,C). These results confirmed that Nef did not actively induce the death of these cells but selectively inhibited the activity of M-CSF.

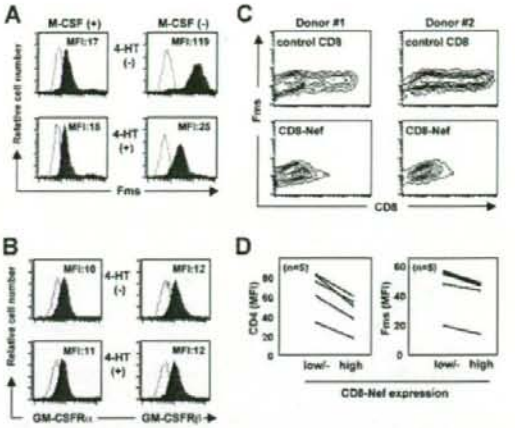

Figure 1. Nef inhibits surface expression of Fms. (A) In the left histograms, TF-1-fms-Nef-ER cells were precultured with M-CSF–containing media in the absence (upper) or presence (lower) of 0.1 mM 4-HT for 24 hours. In the right histograms, TF-1-fms-Nef-ER cells were precultured with M-CSF–free media in the absence (top) or presence (bottom) of 0.1 μM 4-HT for 12 hours. The surface expression of Fms on these cells was analyzed by flow cytometry with PE-labeled anti-Fms antibody. The mean fluorescence intensity (MFI) of Fms expression is indicated. (B) TF-1-Nef ER cells were precultured with GM-CSF–free media in the absence (top) or presence (bottom) of 0.1 μM 4-HT for 12 hours. The surface expression of GM-CSF receptors was analyzed with FITC-labeled anti-α chain (left) and PE-labeled anti-β chain (right) antibodies. The MFI of GM-CSF receptor expression is indicated. (C) Macrophages were nucleofected with the control CD8 plasmid or CD8-Nef plasmid and then costained with APC-labeled anti-CD8 and PE-labeled anti-Fms. Results with macrophages obtained from 2 different donors are shown as contour plots. (D) As in panel C, the nucleofected macrophages were costained with APC-labeled anti-CD8 and PE-labeled anti-Fms, or with APC-labeled anti-CD8 and PE-labeled anti-CD4. The MFI of the expression of Fms or CD4 in the populations of $CD8^{low/-}$, $CD8^{high}$, $CD8\text{-}Nef^{low/-}$, or $CD8\text{-}Nef^{high}$ was analyzed. The results with macrophages obtained from 5 different donors are summarized.

Next, we carefully examined whether Nef down-regulated the surface expression of Fms, as a possible mechanism for the selective inhibitory effect of Nef on the activity of M-CSF. In a previous study in which TF-1-fms-Nef-ER cells cultured under M-CSF–containing conditions were used, we failed to observe an obvious down-regulation of Fms expression by Nef.[26] However, the effect of Nef might have been underestimated under such conditions, because M-CSF itself down-regulated the expression by inducing the internalization/degradation of Fms.[43] Indeed, the addition of M-CSF caused the down-regulation of Fms in both TF-1-fms-Nef-ER cells (Figure S2A) and primary macrophages (Figure S2B) in a dose-dependent manner and an obvious effect of Nef on the surface level of Fms was not detected under such conditions (Figure 1A left panels). However, under the M-CSF–free Fms-high conditions, a significant reduction in the surface expression of Fms was observed in the Nef-active TF-1-fms-Nef-ER cells (Figure 1A right panels). The surface expression of CD29 (integrin β1), CD33, and CD54 (ICAM-1) was unaffected by the same treatment (data not shown). Furthermore, such down-regulation was not observed with the α chain and β chain of GM-CSF receptors (Figure 1B). Thus, the inhibitory effect of Nef on the activity of M-CSF but not of GM-CSF was likely to be due to the selective down-regulation of Fms expression.

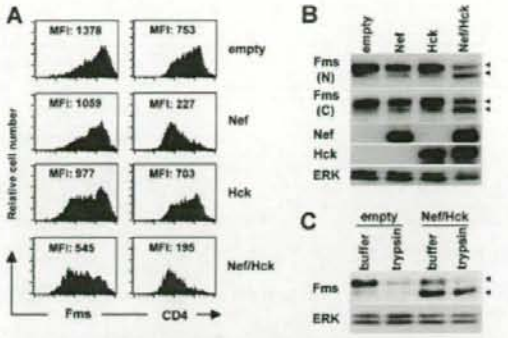

Figure 2. Nef reduces surface expression of Fms in 293 cells and increases intracellular gp130Fms, in the presence of Hck. (A) In the left panels, parental 293 cells were transfected with the Fms plasmid, alone or in combination with the plasmid for Nef (CD8-Nef) or Hck (IRES-EGFP), and then stained with PE-labeled anti-Fms. In the right panels, 293 cells stably expressing CD4 were transfected with the indicated plasmids and stained with PE-labeled anti-CD4. These cells were costained with APC-labeled anti-CD8, and the data for cells positive for both CD8 and EGFP are shown. The MFI of the expression of Fms or CD4 is indicated. (B) As in panel A, parental 293 cells were transfected with the Fms plasmid, alone or in combination with the plasmid for Nef or Hck. Total cell lysate was prepared and subjected to Western blotting with antibodies against the N-terminal portion of Fms (N), the C-terminal portion of Fms (C), Hck, Nef, or ERK. (C) 293 cells stably expressing Fms were cotransfected with Nef and Hck (Nef/Hck), or transfected with empty vectors (empty), and then treated with trypsin or control buffer. Total cell lysate was prepared and subjected to Western blotting with antibodies against the C-terminal portion of Fms or ERK. (B,C) The ERK blot is a loading control. The ◀ indicate the position of gp150Fms or gp130Fms.

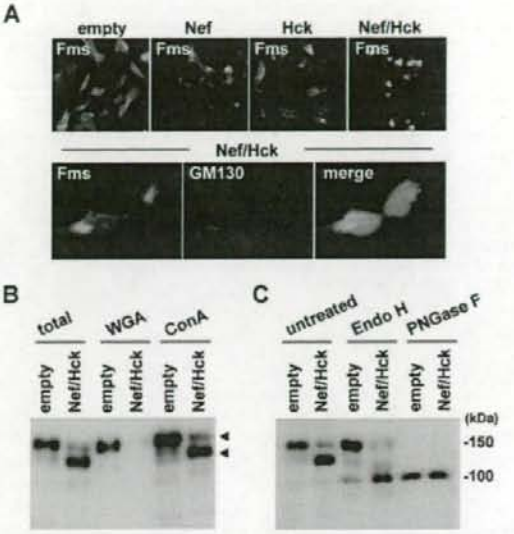

Figure 3. gp130Fms appearing in 293 cells coexpressing Nef/Hck is Golgi-localized underglycosylated Fms. (A) 293 cells stably expressing Fms were transfected with the control CD8 plasmid (empty) or CD8-Nef plasmid (Nef). Similarly, 293 cells stably coexpressing Fms and Hck were transfected with the control CD8 plasmid (Hck) or CD8-Nef plasmid (Nef/Hck). These cells were stained with anti-Fms antibody (top panels). In the bottom panels, 293 cells stably coexpressing Fms and Hck were transfected with CD8-Nef and costained with anti-Fms antibody (green), anti-GM130 antibody (red), and DAPI (blue). (B) 293 cells stably expressing Fms were cotransfected with Nef and Hck (Nef/Hck), or transfected with empty vectors (empty). The total cell lysate was subjected to Fms Western blotting directly (total) or after pull down with WGA-agarose or Con A–agarose. The arrowheads indicate the position of gp150Fms or gp130Fms. (C) Total cell lysate prepared as in panel B was subjected to Fms Western blotting directly (untreated) or after treatment with endo-β-*N*-acetylglucosaminidase H (Endo H) or peptide-*N*-glycosidase F (PNGase F).

The novel function of Nef was further confirmed by nucleofecting Nef into human primary macrophages (Figure 1C,D). The purity of the macrophage preparations was usually more than 95% and 85% when assessed by the expression of CD14 and Fms, respectively (Figure S3). We used the CD8-Nef plasmid encoding Nef fused to the extracellular/transmembrane regions of CD8[34] to identify Nef-positive macrophages. The nucleofection of the control CD8 plasmid encoding only those regions of CD8 did not affect the expression of Fms (Figure 1C "control CD8" panels). In contrast, in the CD8-Nef–nucleofected macrophages, the Fms^{high} population was reduced as the expression of CD8-Nef increased (Figure 1C "CD8-Nef" panels). Such down-regulation of Fms as well as CD4 in the CD8-Nef^{high} population was reproducibly observed with macrophages derived from different donors (Figure 1D). The supernatant obtained from macrophages nucleofected with the CD8-Nef plasmid did not affect the level of Fms in TF-1-fms cells (data not shown), suggesting that production of M-CSF, if any occurred, was not involved in the Nef-induced down-regulation of Fms in macrophages.

Down-regulation of Fms by Nef is Hck-dependent and due to inhibition of intracellular maturation/trafficking of Fms

As both TF-1-fms cells[26] and macrophages[16] endogenously expressed Hck, it was possible that Hck was involved in the down-regulation of Fms caused by Nef. To examine this possibility and clarify the molecular mechanisms by which Nef down-regulated Fms, we next performed a transfection experiment using human 293 cells. As shown (Figure 2A left panels), the cotransfection of Nef and Hck markedly reduced the surface expression of Fms, although the transfection of Nef alone or Hck alone was effective to a certain degree. This was in contrast with the finding that the transfection of Nef alone was almost sufficient to reduce the surface expression of CD4 (Figure 2A right panels). The reduced surface expression of Fms was confirmed by Western blotting. As shown (Figure 2B), the amount of Fms species with a molecular weight of 150 kDa (gp150Fms, upper arrowhead) in the cells coexpressing Nef/Hck was obviously less than that in cells expressing Nef alone or Hck alone. Indeed, gp150Fms was the cell surface form of Fms, because the treatment of the cell surface with trypsin resulted in the loss of gp150Fms (Figure 2C). The trypsin-resistant gp150Fms might represent an intracellular pool of mature Fms that would be rapidly inserted into the plasma membrane. Interestingly, in parallel with the decrease in the expression of gp150Fms, an increase in the expression of a lower molecular weight species (130 kDa, lower arrowheads) was observed in the cells coexpressing Nef/Hck (Figure 2C). The 130-kDa species was a Fms-related product, because the 2 antibodies against the different portions of Fms (the N-terminus and C-terminus) detected the species (herein referred to as gp130Fms). In contrast to gp150Fms, gp130Fms was an intracellular form of Fms, because it was unaffected by the trypsin treatment (Figure 2C). Thus, the down-regulation of Fms observed in TF-1-fms-Nef-ER cells and macrophages was reproducible in 293 cells cotransfected with Nef and Hck, and associated with the increase of the intracellular gp130Fms.

To further characterize the intracellular gp130Fms that appeared in the cells coexpressing Nef/Hck, we next performed immunofluorescence microscopy. As shown (Figure 3A top panels; Figure S4 top panels), the pattern of Fms staining in the coexpressing cells was quite different from that in cells expressing Nef alone

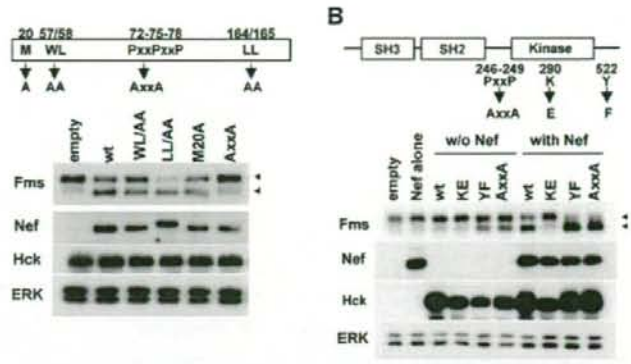

Figure 4. Activation of Hck by Nef is essential but not sufficient for accumulation of gp130Fms. (A) The Nef mutants used (M20A, WL/AA, AxxA, and LL/AA) are schematically shown. All the constructs are CD8-Nef chimeras. 293 cells stably expressing Fms were cotransfected with wild-type Hck and the plasmid indicated, and then analyzed for the expression of Fms, Nef, Hck, or ERK by Western blotting. (B) Schematic representations of Hck and the mutants used. KE is the kinase-dead form, whereas AxxA and YF are the constitutive-active forms.[14] 293 cells stably expressing Fms were transfected with empty vectors (empty), Nef plasmid (Nef), or the indicated Hck plasmid ("w/o Nef" lanes), or cotransfected with wild-type Nef and the indicated Hck plasmid ("with Nef" lanes). Then, the transfected cells were analyzed for the expression of Fms, Nef, Hck, or ERK by Western blotting. (A,B) The ERK blot is a loading control. The ◀ indicate the position of gp150Fms or gp130Fms.

or Hck alone. In a significant proportion of the cells coexpressing Nef/Hck, intense staining of Fms was detected in a perinuclear compartment (Figure 3A top Nef/Hck panel), which largely overlapped the signal for GM130, a marker for the Golgi apparatus[44] (Figure 3A bottom panels) and that for Vti1a, another Golgi marker[45] (Figure S4). Such intense staining of Fms in the perinuclear compartment was also detected in a few cells transfected with Nef alone or Hck alone (Figure 4A; Figure S4), which overlapped the signal for GM130 (Figure S4). Thus, it was highly likely that gp130Fms appeared in the coexpressing cells predominantly localized to the Golgi. As the N-glycosylation of many glycoproteins including Fms is known to be intimately linked with intracellular trafficking,[46-50] we then analyzed the state of the N-glycosylation of gp130Fms. For this purpose, we used 2 lectins, WGA and Con A, which recognize sialic acid and mannose, respectively.[39] As shown (Figure 3B), both gp150Fms and gp130Fms bound to Con A, whereas only gp150Fms bound to WGA, indicating that gp150Fms was modified with both mannose and sialic acid, but gp130Fms was not modified with sialic acid. Indeed, gp150Fms and gp130Fms showed similar electrophoretic mobility following the complete digestion of oligosaccharide groups by PNGase F, whereas only gp130Fms was sensitive to Endo-H, which selectively cleaves high-mannose type oligosaccharides (Figure 3C). These results suggested that the difference in their sizes was due to a difference in the N-glycosylation. Given that nascent Fms polypeptides are modified initially with mannose at the endoplasmic reticulum and terminally with sialic acid at the Golgi,[46-49] our results strongly suggested that the Nef/Hck-dependent accumulation of gp130Fms at the Golgi was due to the perturbation of intracellular N-glycosylation and/or trafficking of nascent Fms.

Down-regulation of Fms by Nef is dependent on activation of Hck and spatial regulation of active Hck

We next attempted to clarify the role of Hck in the down-regulation of Fms expression by Nef. Initially, we examined whether the direct interaction with Hck (Figure S5) was required for the function of Nef, using Nef mutants. As shown (Figure 4A), the AxxA mutant defective in the interaction with Hck[12] failed to down-regulate Fms, that is, the decrease of gp150Fms and the concomitant increase of gp130Fms. In contrast, the other 3 mutants still down-regulated Fms (Figure 4A). The WL/AA and LL/AA mutants, and the M20A mutant were shown to be defective in the down-regulation of CD4 and MHC I, respectively,[24,37] which was confirmed in our experimental system (data not shown). These results suggested that the down-regulation of Fms by Nef was mechanistically different from that of CD4 or MHC I, and dependent on the direct interaction with Hck. Thus, we next examined whether the activation of Hck by Nef was necessary and sufficient for the down-regulation of Fms, using Hck mutants. As shown (Figure 4B), Nef failed to down-regulate Fms when cotransfected with the kinase-dead KE mutant, but almost completely down-regulated Fms when cotransfected with the YF or AxxA mutant, both of which were the constitutive-active form. However, it should be noted that the transfection of these constitutive-active forms of Hck alone was not necessarily sufficient to achieve the full down-regulation of Fms (Figure 4B, see YF, AxxA, wt + Nef, YF + Nef, and AxxA + Nef lanes). These results clearly indicated that the activation of Hck was necessary but not sufficient for the Nef/Hck-induced down-regulation of Fms.

It has been shown that Nef distributes to the Golgi as well as the plasma membrane.[22,24] Indeed, intense signal of the CD8-Nef chimera was detected in the perinuclear compartment, which overlapped the signal for GM130 (Figure 5A). Thus, it was possible that the activation of Hck at the Golgi or the recruitment of the active Hck to the Golgi was another factor necessary for Nef to down-regulate Fms. To explore this possibility, we examined whether the active Hck in the Nef-expressing cells indeed localized to the Golgi and its existence at the Golgi correlated with the down-regulation of Fms. To detect the active Hck, we stained cells with the antibody specific for Hck phosphorylated at Tyr411, which was the major autophosphorylation site.[14] As shown (Figure 5B), an intense signal for the active Hck was indeed detected in the perinuclear compartment, in cells coexpressing Nef and wild-type Hck but not in cells expressing wild-type Hck alone (top panels), which largely overlapped the signal for GM130 (middle panels). Such colocalization of Nef and active Hck in the perinuclear compartment was also observed in macrophages nucleofected with the CD8-Nef plasmid (Figure S6). Moreover, the constitutive-active AxxA Hck tended to localize to the perinuclear compartment when expressed alone, and almost exclusively localized to the perinuclear compartment when coexpressed with Nef (Figure 5B bottom panels). Thus, the degree to which the active Hck accumulated at the Golgi correlated well with the observed down-regulation of Fms (Figure 4B). Taken together, these results suggest that the novel function of Nef (ie, the down-regulation of Fms expression by perturbing the maturation/trafficking of nascent Fms) is dependent on both the activation of Hck and the spatial regulation of the active Hck.

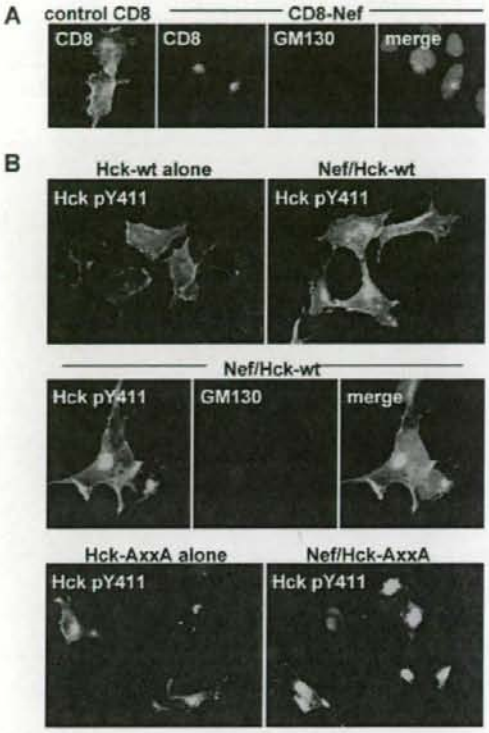

Figure 5. Nef induces Golgi localization of active Hck. (A) Parental 293 cells were transfected with the control CD8 plasmid or CD8-Nef plasmid, and then stained with anti-CD8 antibody (green), anti-GM130 antibody (red), or DAPI (blue). (B) In the top panels, parental 293 cells were transfected with wild-type Hck, or cotransfected with wild-type Hck and Nef, and then stained with the antibody specific for active Hck (ie, Hck phosphorylated at Tyr411). In the middle panels, parental 293 cells cotransfected with wild-type Hck and Nef were costained with anti-Hck pTyr411 antibody (green), anti-GM130 antibody (red), and DAPI (blue). In the bottom panels, parental 293 cells were transfected with the constitutive-active AxxA Hck (see Figure 4B), or cotransfected with the AxxA Hck and wild-type Nef, and then stained with anti-Hck pTyr411 antibody. See "Western blotting, flow cytometry, and immunofluorescence with 293 cells" for image acquisition information.

Discussion

In this study, we showed for the first time that Nef down-regulated the expression of Fms (Figures 1,2). The down-regulation was due to perturbation of the intracellular trafficking of nascent Fms (Figure 3), and likely to be a cause of the inhibitory effect of Nef on the activity of M-CSF because neither the activity of GM-CSF nor the cell surface expression of GM-CSF receptors was inhibited by Nef (Figure 1). Importantly, the present study strongly suggested that the down-regulation of Fms expression by Nef was due to a previously unreported mechanism that depended on both the activation of Hck and the aberrant spatial regulation of the active Hck (Figures 4,5).

The Nef-induced down-regulation of Fms was obviously mechanistically different from that of CD4 or MHC I in its dependence on Hck (Figures 2A,3A)[6,7,20-23] but appeared to resemble that of HFE. The Nef-induced down-regulation of HFE was abolished by either a mutation in the PxxP motifs of Nef or the overexpression of the dominant-negative Hck.[24] However, how Hck was involved in the Nef-induced down-regulation of HFE remains to be analyzed.[24] Interestingly, the YxxA motif in the cytoplasmic tail of HFE (^{342}YVLA) was shown to be required for Nef to down-regulate HFE.[24] The tyrosine-based YxxA motif was conserved in the kinase domain of Fms (^{873}YQMA, GenBank accession number P07333). However, when coexpressed with Hck, Nef also down-regulated a Fms mutant lacking the motif prepared by introducing the stop codon at ^{873}Y (data not shown). Thus, the mechanism for the Nef/Hck-induced down-regulation of Fms was likely to be somewhat different from that of HFE. Our earlier experiment revealed that gp130Fms was tyrosine phosphorylated in cells coexpressing Nef and Hck.[26] However, the ligand-independent tyrosine phosphorylation of Fms was not a direct cause of the down-regulation of Fms, because Nef also down-regulated a Fms mutant lacking the entire intracellular region when coexpressed with Hck (Figure S7).

The Nef/Hck-induced down-regulation of Fms was associated with the accumulation of the immature Fms at the Golgi (Figure 3). The experiment with Hck mutants clearly demonstrated that the activation of Hck was indispensable for the down-regulation of Fms (Figure 4B). The finding that Nef failed to down-regulate Fms when coexpressed with Lyn or Fgr (data not shown) further supported the conclusion, because Hck was the only Src kinase activated by Nef among Src kinases highly expressed in macrophages (ie, Hck, Lyn, and Fgr).[13-16] However, to our surprise, the activation of Hck was not the sole determinant of the down-regulation of Fms, because the expression of the constitutive-active Hck (YF or AxxA) alone was insufficient to fully achieve the down-regulation (Figure 4B). Our finding that the degree to which the active Hck accumulated at the Golgi correlated well with that of the down-regulation of Fms (Figures 4B,5B) strongly suggested that Nef down-regulated Fms through both the activation of Hck and the accumulation of the active Hck at the Golgi. The idea may answer why Hck, the downstream effector molecule important for the Fms signaling pathways,[38,50-53] is involved in the down-regulation of Fms by Nef.

A significant pool of Nef has been shown to localize to the Golgi.[22,24] Indeed, the CD8-Nef chimera used in this study localized to the Golgi as well as the plasma membrane (Figure 5A). This was not due to the fusion of the region of CD8 to the N-terminus of Nef, because the Nef-EGFP chimera, in which EGFP was fused to the C-terminus of Nef, also localized to the Golgi (data not shown). Thus, it was likely that the interaction with the Golgi-resident Nef or the recruitment of the active Hck led to the accumulation of the active Hck at the Golgi. However, it is unclear how this accumulation leads to a block of the intracellular trafficking of Fms in the same compartment. A plausible possibility might be direct interaction of the active Hck with Fms at the Golgi. Indeed, our earlier coimmunoprecipitation experiment revealed the formation of a molecular complex between Hck and Fms.[26] Meanwhile, it is known that the tyrosine located in the juxtamembrane domain of Fms (Y561 in human and Y559 in murine) serves as a binding site for Src kinases including Hck when the residue is autophosphorylated.[51-54] However, when coexpressed with Hck, Nef also down-regulated a Fms mutant in which the tyrosine residue was replaced with phenylalanine (data not shown). Thus, the active Hck at the Golgi may interact with Fms via unidentified site(s) or form complexes with Fms indirectly. Another possibility might be an alteration of the Golgi structure caused by the accumulation of the active Hck at the compartment. Recent studies revealed that Src kinases including Hck were present on the Golgi membrane as well as the plasma membrane.[55-57] The importance of the Golgi-localized Src kinases for the maintenance of the Golgi structure was clearly demonstrated by the finding that SYF

fibroblasts lacking the 3 ubiquitous Src kinases (Src, Yes, and Fyn) exhibited an aberrant morphology of the Golgi with collapsed stacks and bloated cisternae.[58] Interestingly, it was also demonstrated that the exogenous expression of the constitutive-active Src (E378G) in the SYF cells affected the distribution of some if not all Golgi-specific proteins.[58] Thus, it is possible that the accumulation of the active Hck affects the structure of the Golgi and thereby perturbs the trafficking of Fms.

A study with HIV-1 transgenic mice has clearly proved the importance of the interaction of Nef with Hck in macrophages for the development of AIDS.[11] Nevertheless, the functional consequences of the Nef/Hck interaction are not fully understood. The activation of Hck induced by the direct interaction with Nef is basically thought to cause the activation of macrophages, which may favor the replication of HIV-1. Indeed, Komuro et al demonstrated that the expression of Hck at a high level in macrophages correlated well with high titer replication of HIV-1.[59] Moreover, Briggs et al raised the possibility that the Nef-Hck interaction caused the activation of the Stat3 transcription factor, thereby mimicking the signaling pathway of the GM-CSF receptor.[25] However, the present study revealed that the Nef/Hck interaction also played a negative role: the molecular interaction caused the down-regulation of Fms and inhibition of the activity of M-CSF, which is likely to be due to the aberrant spatial regulation of the active Hck. The differential modulation of the activities of GM-CSF and M-CSF by Nef may alter the profile of production of cytokine/chemokines in HIV-1–infected macrophages, contributing to the development of AIDS. Future studies will clarify whether small compounds specifically targeting the Nef-Hck interaction prevent the progression of the disease. Moreover, a detailed mechanistic analysis of the unique function of Nef will help us to understand how Fms and Src kinases tightly regulate the signaling pathways and functions of macrophages.

Acknowledgments

We thank Y. Endo for secretarial assistance.

This work was supported in part by Health and Labor Sciences Research Grants from the Ministry of Health, Labor and Welfare of Japan (S.O., S.S.).

Authorship

Contribution: M.H. and S.S. were responsible for the overall experimental work and design; Y.Y. and H.A., for DNA cloning; R.H., for Western blotting; H.H., for flow cytometry; N.S., for immunofluorescence; K.M. and S.O., for project planning and data analysis.

M.H. and S.S. contributed equally to this study.

Conflict-of-interest disclosure: The authors declare no competing financial interests.

Correspondence: Seiji Okada, Division of Hematopoiesis, Center for AIDS Research, Kumamoto University, Honjo 2-2-1, Kumamoto-city, Kumamoto 860-0811, Japan; e-mail: okadas@gpo.kumamoto-u.ac.jp.

References

1. Pantaleo G, Fauci AS. Immunopathogenesis of HIV infection. Annu Rev Microbiol. 1996;50:825-854.
2. Stevenson M. HIV-1 pathogenesis. Nat Med. 2003;9:853-860.
3. Letvin NL, Walker BD. Immunopathogenesis and immunotherapy in AIDS virus infections. Nat Med. 2003;9:861-866.
4. Kedzierska K, Crowe SM. Cytokines and HIV-1: interactions and clinical implications. Antivir Chem Chemother. 2001;12:133-150.
5. Maslin CLV, Kedzierska K, Webster NL, Muller WA, Crowe SM. Transendothelial migration of monocytes: underlying molecular mechanisms and consequences of HIV-1 infection. Curr HIV Res. 2005;3:303-317.
6. Fackler OT, Baur AS. Live and let die: Nef functions beyond HIV replication. Immunity. 2002;16:493-497.
7. Peterlin BM, Trono D. Hide, shield and strike back: how HIV-infected cells avoid immune eradication. Nat Rev Immunol. 2003;3:97-107.
8. Kirchhoff F, Greenough TC, Brettler DB, Sullivan JL, Desrosiers RC. Brief report: absence of intact nef sequences in a long-term survivor with nonprogressive HIV-1 infection. N Engl J Med. 1995;332:228-232.
9. Deacon NJ, Tsykin A, Solomon A, et al. Genomic structure of an attenuated quasi species of HIV-1 from a blood transfusion donor and recipients. Science. 1995;270:988-991.
10. Hanna Z, Kay DG, Rebai N, Guimond A, Jothy S, Jolicoeur P. Nef harbors a major determinant of pathogenicity for an AIDS-like disease induced by HIV-1 in transgenic mice. Cell. 1998;95:163-175.
11. Hanna Z, Weng X, Kay DG, Poudrier J, Lowell C, Jolicoeur P. The pathogenicity of human immunodeficiency virus (HIV) type 1 Nef in CD4C/HIV transgenic mice is abolished by mutation of its SH3-binding domain, and disease development is delayed in the absence of Hck. J Virol. 2001;75:9378-9392.
12. Saksela K, Cheng G, Baltimore D. Proline-rich (PxxP) motifs in HIV-1 Nef bind to SH3 domains of a subset of Src kinases and are required for the enhanced growth of Nef+ viruses but not for down-regulation of CD4. EMBO J. 1995;14:484-491.
13. Moarefi I, LaFevre-Bernt M, Sicheri F, et al. Activation of the Src-family tyrosine kinase Hck by SH3 domain displacement. Nature. 1997;385:650-653.
14. Lerner EC, Smithgall TE. SH3-dependent stimulation of Src-family kinase autophosphorylation without tail release from the SH2 domain in vivo. Nat Struct Biol. 2002;9:365-369.
15. Briggs SD, Lerner EC, Smithgall TE. Affinity of Src family kinase SH3 domains for HIV Nef in vitro does not predict kinase activation by Nef in vivo. Biochemistry. 2000;39:489-495.
16. Lowell CA. Src-family kinases: rheostats of immune signaling. Mol Immunol. 2004;41:631-643.
17. Bromann PA, Korkaya H, Courtneidge SA. The interplay between Src family kinases and receptor tyrosine kinases. Oncogene. 2004;23:7957-7968.
18. Zhang H, Meng F, Chu CL, Takai T, Lowell CA. The Src family kinases Hck and Fgr negatively regulate neutrophil and dendritic cell chemokine signaling via PIR-B. Immunity. 2005;22:235-246.
19. Mermel CH, McLemore ML, Liu F, et al. Src family kinases are important negative regulators of G-CSF-dependent granulopoiesis. Blood. 2006;108:2562-2568.
20. Garcia JV, Miller AD. Serine phosphorylation-independent downregulation of cell-surface CD4 by nef. Nature. 1991;350:508-511.
21. Schwartz O, Marechal V, Le Gall S, Lemonnier F, Heard JM. Endocytosis of major histocompatibility complex class I molecules is induced by the HIV-1 Nef protein. Nat Med. 1996;2:338-342.
22. Greenberg ME, Iafrate AJ, Skowronski J. The SH3 domain-binding surface and an acidic motif in HIV-1 Nef regulate trafficking of class I MHC complexes. EMBO J. 1998;17:2777-2789.
23. Williams M, Roeth JF, Kasper MR, Filzen TM, Collins KL. Human immunodeficiency virus type 1 Nef domains required for disruption of major histocompatibility complex class I trafficking are also necessary for coprecipitation of Nef with HLA-A2. J Virol. 2005;79:632-636.
24. Drakesmith H, Chen N, Ledermann H, Screaton G, Townsend A, Xu XN. HIV-1 Nef down-regulates the hemochromatosis protein HFE, manipulating cellular iron homeostasis. Proc Natl Acad Sci U S A. 2005;102:11017-11022.
25. Briggs SD, Scholtz B, Jacque J-M, Swingler S, Stevenson M, Smithgall TE. HIV-1 Nef promotes survival of myeloid cells by a Stat3-dependent pathway. J Biol Chem. 2001;276:25605-25611.
26. Suzu S, Harada H, Matsumoto T, Okada S. HIV-1 Nef interferes with M-CSF receptor signaling through Hck activation and inhibits M-CSF bioactivities. Blood. 2005;105:3230-3237.
27. Gasson J. Molecular physiology of granulocyte-macrophage colony-stimulating factor. Blood. 1991;77:1131-1145.
28. Roth P, Stanley ER. The biology of CSF-1 and its receptor. Curr Top Microbiol Immunol. 1992;181:141-167.
29. Hashimoto S, Suzuki T, Dong HY, Yamazaki N, Matsushima K. Serial analysis of gene expression in human monocytes and macrophages. Blood. 1999;94:837-844.
30. Kitamura T, Tange T, Terasawa T, et al. Establishment and characterization of a unique human cell line that proliferates dependently on GM-CSF, IL-3, or erythropoietin. J Cell Physiol. 1989;140:323-334.

31. Suzu S, Kimura F, Ota J, et al. Biologic activity of proteoglycan macrophage colony-stimulating factor. J Immunol. 1997;159:1860-1867.
32. Walk SF, Alexander M, Maier B, Hammarskjold M-L, Rekosh DM, Ravichandran KS. Design and use of an inducibly activated immunodeficiency virus type 1 Nef to study immune modulation. J Virol. 2001;75:834-843.
33. Shugars DC, Smith MS, Glueck DH, Nantermet PV, Seillier-Moiseiwitsch F, Swanstrom R. Analysis of human immunodeficiency virus type 1 nef gene sequences present in vivo. J Virol. 1993;67: 4639-4650.
34. Sawai ET, Baur A, Struble H, Peterlin BM, Levy JA, Cheng-Mayer C. Human immunodeficiency virus type 1 Nef associates with a cellular serine kinase in T lymphocytes. Proc Natl Acad Sci U S A. 1994;91:1539-1543.
35. Murakami Y, Fukazawa H, Kobatake T, et al. A mammalian two-hybrid screening system for inhibitors of interaction between HIV Nef and the cellular tyrosine kinase Hck. Antiviral Res. 2002; 55:161-168.
36. Tahara-Hanaoka S, Ushijima Y, Tarui H, et al. Differential level of co-down-modulation of CD4 and CXCR4 promed by HIV-1 gp120 in response to phorbol ester, PMA, among HIV-1 isolates. Microbiol Immunol. 2000;44:489-498.
37. Akari H, Arold S, Fukumori T, Okazaki T, Strebel K, Adachi A. Nef-induced major histocompatibility complex class I down-regulation is functionally dissociated from its virion incorporation, enhancement of viral infectivity, and CD4 down-regulation. J Virol. 2000;74:2907-2912.
38. Suzu S, Tanaka-Douzono M, Nomaguchi K, et al. $p56^{dok-2}$ as a cytokine-inducible inhibitor of cell proliferation and signal transduction. EMBO J. 2000;19:5114-5122.
39. Spivak JL, Avedissian LS, Pierce JH, Williams D, Hankins WD, Jensen RA. Isolation of the full-length murine erythropoietin receptor using a baculovirus expression system. Blood. 1996;87: 926-937.
40. Schmidt-Arras DE, Bohmer A, Markova B, Choudhary C, Serve H, Bohmer F. Tyrosine phosphorylation regulates maturation of receptor tyrosine kinases. Mol Cell Biol. 2005;25:3690-3703.
41. Xiang Z, Kreisel F, Cain J, Colson A, Tomasson MH. Neoplasia driven by mutant c-KIT by intracellular, not plasma membrane, receptor signaling. Mol Cell Biol. 2007;27:267-282.
42. Suzu S, Hiyoshi M, Yoshidomi Y, et al. M-CSF-mediated macrophage differentiation but not proliferation is correlated with increased and prolonged ERK activation. J Cell Physiol. 2007;212: 519-525.
43. Lee PS, Wang Y, Dominguez MG, et al. The Cbl protooncogene stimulates CSF-1 receptor multiubiquitination and endocytosis, and attenuates macrophage proliferation. EMBO J. 1999;18: 3616-3628.
44. Puthenveedu MA, Bachert C, Puri S, Lanni F, Linstedt AD. GM130 and GRASP65-dependent lateral cisternal fusions allows uniform Golgi-enzyme distribution. Nat Cell Biol. 2006;8:238-248.
45. Xu Y, Wong SH, Tang BL, Subramaniam VN, Zhang T, Hong W. A 29-kilodalton Golgi soluble N-ethylmaleimide-sensitive factor attachment protein receptor (Vti1-rp2) implicated in protein trafficking in the secretory pathway. J Biol Chem. 1998;273:21783-21789.
46. Helenius A, Aebi M. Intracellular functions of N-linked glycans. Science. 2001;291:2364-2369.
47. Sherr CJ, Rettenmier CW, Sacca R, Roussel MF, Look AT, Stanley ER. The c-fms proto-oncogene product is related to the receptor for the mononuclear phagocyte growth factor, CSF-1. Cell. 1985;41:665-676.
48. Roussel MF, Downing JR, Rettenmier CW, Sherr CJ. A point mutation in the extracellular domain of the human CSF-1 receptor (c-fms proto-oncogene product) activates its transforming potential. Cell. 1988;55:979-988.
49. Woolford J, McAuliffe A, Rohrschneider LR. Activation of the feline c-fms proto-oncogene: multiple alterations are required to generate a fully transformed phenotype. Cell. 1988;55:865-977.
50. Sherr CJ. Colony-stimulating factor-1 receptor. Blood. 1990;75:1-12.
51. Courtneidge SA, Dhand R, Pilat D, Twamley GM, Waterfield MD, Roussel MF. Activation of Src family kinases by colony stimulating factor-1, and their association with its receptor. EMBO J. 1993; 12:943-950.
52. Alonso G, Koegl M, Mazurenko N, Courtneidge SA. Sequence requirements for binding of Src family tyrosine kinases to activated growth factor receptors. J Biol Chem. 1995;270:9840-9848.
53. Marks DC, Csar XF, Wilson NJ, et al. Expression of a Y559F mutant CSF-1 receptor in M1 myeloid cells: a role for Src kinases in CSF-1 receptor-mediated differentiation. Mol Cell Biol Res Commun. 1999;1:144-152.
54. Rohde CM, Schrum J, Lee AWM. A juxtamembrane tyrosine in the colony-stimulating factor-1 receptor regulates ligand-induced Src association, receptor kinase function, and down-regulation. J Biol Chem. 2004;279:43448-43461.
55. Carreno S, Gouze M, Schaak S, Emorine LJ, Maridonneau-Parini I. Lack of palmitoylation redirects $p59^{Hck}$ from the plasma membrane to $p61^{Hck}$-positive lysosomes. J Biol Chem. 2000; 275:36223-36229.
56. Chiu VK, Bivona T, Hach A, et al. Ras signaling on the endoplasmic reticulum and the Golgi. Nat Cell Biol. 2002;4:343-350.
57. Kasahara K, Nakayama Y, Ikeda K, et al. Trafficking of Lyn through the Golgi caveolin involves the charged residues on αE and αI helices in the kinase domain. J Cell Biol. 2004;165:641-652.
58. Bard F, Mazelin L, Pechoux-Longin C, Malhorta V, Jurdic P. Src regulates Golgi structure and KDEL receptor-dependent retrograde transport to the endoplasmic reticulum. J Biol Chem. 2003;47: 46601-46606.
59. Komuro I, Yokota Y, Yasuda S, Iwamoto A, Kagawa KS. Regulation of Hck and C/EBPβ represent a heterogeneous susceptibility of monocyte-derived macrophages to M-tropic HIV-1 infection. J Exp Med. 2003;198:443-453.

J. Parasitol., 94(5), 2008, pp. 1128–1138

PREVALENCE AND MOLECULAR PHYLOGENETIC CHARACTERIZATION OF *TRYPANOSOMA* (*MEGATRYPANUM*) *MINASENSE* IN THE PERIPHERAL BLOOD OF SMALL NEOTROPICAL PRIMATES AFTER A QUARANTINE PERIOD

Hiroshi Sato, Natalie Leo, Yuko Katakai*†, Jun-ichiro Takano*, Hirofumi Akari†, Shin-ichiro Nakamura‡, and Yumi Une‡

Laboratory of Veterinary Parasitology, Faculty of Agriculture, Yamaguchi University, 1677-1 Yoshida, Yamaguchi 753-8515, Japan. *e-mail: sato7dp4@yamaguchi-u.ac.jp*

ABSTRACT: Neotropical primates of the Cebidae and Callitrichidae, in their natural habitats, are frequently infected with a variety of trypanosomes including *Trypanosoma cruzi*, which causes a serious zoonosis, Chagas' disease. The state of trypanosome infection after a 30-day quarantine period was assessed in 85 squirrel monkeys (*Saimiri sciureus*) and 15 red-handed tamarins (*Saguinus midas*), that were wild-caught and exported to Japan as companion animals or laboratory animals, for biomedical research, respectively. In addition to many microfilariae of *Mansonella* (*Tetrapetalonema*) *mariae* at a prevalence of 25.9%, and *Dipetalonema caudispina* at a prevalence of 3.5%, a few trypomastigotes of *Trypanosoma* (*Megatrypanum*) *minasense* were detected in Giemsa-stained thin films of blood from 20 squirrel monkeys at a prevalence of 23.5%. Although few *T. minasense* trypomastigotes were found in Giemsa-stained blood films from tamarins, a buffy-coat examination detected trypanosomes in 12 red-handed tamarins (80.0%), and PCR amplification of a highly variable region of the small subunit ribosomal RNA genes (SSU rDNA) for *Trypanosoma* spp. detected the infection in 14 of the 15 tamarins (93.3%). Nucleotide sequences of the amplicons were identical for trypanosomes from tamarins and squirrel monkeys, indicating a high prevalence but low parasitemia of *T. minasense* in imported Neotropical nonhuman primates. Based on the SSU rDNA and 5.8S rDNA, the molecular phylogenetic characterization of *T. minasense* indicated that *T. minasense* is closely related to trypanosomes with *Trypanosoma theileri*-like morphology and is distinct from *Trypanosoma* (*Tejeraia*) *rangeli*, as well as from *T. cruzi*. Using some blood samples from these monkeys, amplification and subsequent sequencing of the glycosomal glyceraldehyde-3-phosphate dehydrogenase (gGAPDH) gene fragments detected 4 trypanosome genotypes, including 2 types of *T. cruzi* clade, 1 type of *T. rangeli* clade, and 1 *T. rangeli*-related type, but failed to indicate its phylogenetic position based on the gGAPDH gene. Furthermore, species ordinarily classified in the *Megatrypanum* by morphological criteria do not form a clade in any molecular phylogenetic trees based on rDNA or gGAPDH genes.

Neotropical primates of the Cebidae and Callitrichidae, such as squirrel monkeys (*Saimiri* spp.), marmosets (*Callithrix* and *Cebuella* spp.), and tamarins (*Saguinus* and *Leontopithecus* spp.), in their natural habitats are frequently infected with a variety of trypanosomes. In addition to 2 zoonotic trypanosome species, i.e., *Trypanosoma* (*Tejeraia*) *rangeri* Téjera, 1920 and *Trypanosoma* (*Schizotrypanum*) *cruzi* Chagas, 1909, Neotropical nonhuman primates are variably infected with *T.* (*Megatrypanum*) *minasense* Chagas, 1909, *T.* (*M.*) *devei* Leger and Porry, 1918, and *T.* (*M.*) *lambretchi* Marinkelle, 1968 (Dunn et al., 1963; Hoare, 1972; Ziccardi et al., 2000). These monkeys are exported to other continents to be kept in research facilities as laboratory animals for biomedical research, e.g., vaccine development for human malaria (WHO, 1988), and in zoo facilities, sometimes as accessible exhibition animals. In addition, small Neotropical monkeys have currently become one of the favorite exotic companion animals in developed countries, including Japan. Although wild-caught monkeys are imported, in most cases, and may have a variety of parasites (Yamashita, 1963; Orihel, 1970; Kuntz and Meyers, 1972; Potkay, 1992; Sullivan et al., 1993), no special attention has been paid to their parasitic infections during the imported-animal quarantine or in sequential animal care under any usages. Exceptionally, an acanthocephalan infection caused by *Prosthenorchis elegans*, which perforates the gut wall, as well as an intestinal nematode infection with *Ptergodermatites nycticebi*, are well known to zoo veterinarians due to a high mortality of the host monkeys (Sato et al., 2003).

The present study reports on the occurrence and prevalence of blood parasites, after a 30-day quarantine period in Japan, in common squirrel monkeys (*Saimiri sciureus*) imported as companion animals and in red-handed tamarins (*Saguinus midas*) imported for use in biomedical research. By examination of stained blood films, we found neither *T. cruzi* nor *T. rangeli* infection, but a high prevalence of *T. minasense* infection, in these monkeys, in addition to microfilariae. Nucleotide sequences of the small and large subunit (SSU/LSU) ribosomal RNA genes (rDNA) of *T. minasense* were determined for the first time. Amplification of the glycosomal glyceraldehyde-3-phosphate dehydrogenase (gGAPDH) detected *T. cruzi* and *T. rangeli* infections in some squirrel monkeys and tamarins, by nested PCR, and a reliable sequence of the *T. minasense* gGAPDH gene was obtained in the present study.

MATERIALS AND METHODS

Parasitological survey

Animals examined in the present study included 85 squirrel monkeys and 15 red-handed tamarins. All of them were wild-caught; the ages of the monkeys were unknown. Furthermore, no information on the original sources, or the periods of captivity, of these monkeys was provided. To quarantine imported primates, they were kept for 30 days in a special facility in the Narita Airport Quarantine. Squirrel monkeys were checked just after this quarantine period, and tamarins were examined after transfer to an experimental animal facility.

The peripheral blood was drawn from squirrel monkeys under inhalation anaesthesia using isoflurane. The main purpose for blood collection at that time was to check antibody levels to viral zoonoses. After making a thin blood film, individual blood samples collected in special tubes for serum separation were centrifuged at 1,300 *g* for 10 min at ambient temperature. After removing the serum, the tubes were then sent, under cool conditions, to the parasitology laboratory. Each tube

Received 26 October 2007; revised 4 December 2007; accepted 27 February 2008.

* The Corporation for Production and Research of Laboratory Primates, 1 Hachimandai, Tsukuba 305-0843, Japan.

† Laboratory of Disease Control, Tsukuba Primate Research Center, National Institute of Biomedical Innovation, 1 Hachimandai, Tsukuba 305-0843, Japan.

‡ Laboratory of Veterinary Pathology, School of Veterinary Medicine, Azabu University, 1-17-71 Fuchinobe, Sagamihara 229-8501, Japan.

contained a coagulated blood mass and a small volume of uncoagulated blood. Parasite DNA extraction was attempted using the latter portion. Initially, samples from tamarins arrived in a similar manner to the ones from squirrel monkeys; however, EDTA-treated blood was later sent to the parasitology laboratory. In addition to preparing thin blood films, EDTA-treated blood was individually aspirated in a capillary hematocrit tube, centrifuged at 1,300 *g* for 10 min at 4 C, and the buffy-coat layer was examined using inverted light microscopy. When trypanosomes were found in the buffy-coat layer, the fine tube was cut to make a smear on a glass slide. Simultaneously, individual blood was used for parasite DNA extraction, as described below.

Morphological examination

Blood films were stained in Giemsa's solution and observed thoroughly at ×200 magnification using light microscopy. Positive blood films with trypanosomes were further observed under oil immersion at ×1,000 magnification. Arbitrarily selected, but undistorted, well-stained trypanosomes, 21 in number from squirrel-monkeys and 6 from tamarins, were photographed at this magnification, transformed into photographs using Adobe® Photoshop® v.5.0 (Adobe Systems, Inc., San Jose, California), and printed out at higher magnification. Measurements were made using printed photographs (×1,413 of the original size on the paper) by use of a digital curvimetre type S (Uchida-yoko, Chuoh-ku, Tokyo, Japan), when necessary. All measurements were expressed in μm and included total length, maximum width, posterior end to middle kinetoplast (PK), kinetoplast to middle of nucleus (KN), middle of nucleus to anterior end (NA), free flagellum (FF), and sizes of kinetoplast and nucleus. Nuclear index (NI) and kinetoplast index (KI) were calculated as follows: NI = (PK + KN)/NA; and KI = (PK + KN)/KN, following Hoare (1972). For comparison with *T. minasense* measurements performed by Ziccardi and Lourenço-de-Oliveira (1999), KI values were also calculated according to Deane and Damasceno (1961), i.e., KI = PK/KN.

DNA extraction, polymerase chain reaction (PCR), and sequencing

Parasite DNA was extracted from 0.2 ml of each blood sample from selected trypanosome- or microfilaria-positive squirrel monkeys, and from all tamarins, using a GFX genomic blood DNA purification kit (Amersham Pharmacia Biotech, Uppsala, Sweden). PCR amplification of a special fragment of the SSU rDNA, used for detecting stercorarian trypanosomes of terrestrial vertebrates, was conducted using a primer pair of TRY927F and TRY927R, and SSU561F and SSU561R (Noyes et al., 1999). Furthermore, amplification of overlapping fragments of the SSU/LSU rDNA of trypanosomes, using multiple primer combinations, was performed using some parasite DNA extracts as described previously (Sato et al., 2005). After direct sequencing of PCR amplicons (Sato et al., 2005), sequences were assembled manually with the aid of the CLUSTRAL W multiple alignment program (Thompson et al., 1994). The SSU/LSU rDNA construction of the trypanosome was determined as described previously (Sato et al., 2005). The gGAPDH gene as amplified with degenerate primers G3 (5′-TTYGCCGYATYGGY CGCATGG-3′) and G5 (5′-ACMAGRTCCACCACRCGGTG-3′) with the following program: 3 min at 95 C followed by 35 cycles of 60 sec at 95 C, 30 sec at 55 C, and 60 sec at 72 C, then a final extension at 72 C for 7 min, according to Hamilton et al. (2004). As sequencing primers, G6 (5′-GYGGTKTCSVTSAAGGACTG-3′) and G7 (5′-CSC CTGTBGTGCTBGGTATG-3′) (Hamilton et al., 2004) were also used. In addition, the gGAPDH gene of *T. cruzi* (Y strain), *T. grosi* (SESUJI and HANTO isolates), and *T. kuseli* (Sato et al., 2005, 2007) were newly sequenced in this study as technical controls. To obtain more gGAPDH genes of trypanosomes from blood samples of squirrel monkeys and tamarins, nested PCR, using a primer pair of G3 and G5 in the first round, and G1 (5′-CGCGGATCCASGGYCTYMTCGGBAM KGAGAT-3′) and G4a (5′-GTTYTGCAGSGTCGCCTTGG-3′) or G1 and G4b (5′-CCAMGASACVAYCTTGAAGAA-3′) primers in the second round, was conducted according to Hamilton et al. (2004). Amplicons were cloned into a plasmid vector pTA2 (Target Clone™; Toyobo, Osaka, Japan) and transformed into *Escherichia coli* JM109 (TOYOBO) according to the instructions of the manufacturer. After propagation, plasmid DNA was extracted by use of a NucleoSpin® Plasmid kit (Macherey-Nagel GmbH, Düren, Germany), and inserts (from at least 3 independent clones per amplicon) were sequenced using M13 forward and reverse primers.

For microfilariae, internal transcribed spacer (ITS) 1 was amplified using the forward primer S.r.ITS1-NC5/F1 (5′-TTACGTCCCTGCCC TTTGTA-3′) and the reverse primer NC13R (5′-GCTGCGTTCTTCA TCGAT-3′) with the following program: 3 min at 95 C followed by 35 cycles of 45 sec at 94 C, 60 sec at 65 C, and 90 sec at 72 C, then a final extension at 72 C for 7 min (Zhu et al., 2000; Sato et al., 2006). PCR products were separated by electrophoresis in 1.3% agarose gels in 0.5 × TBE buffer, stained with ethidium bromide, and visualized under ultraviolet light. To estimate the molecular sizes, 100-bp DNA Ladder (Promega, Madison, Wisconsin) was used. Molecular sizes of PCR products of *T. cruzi* and *T. rangeli* by use of a primer pair of TRY927F and TRY927R were calculated using deposited sequences in the DDBJ/EMBL/GenBank databases under the accession numbers AF228685, AF232214, AF239980, AF239981, AF245380–AF245383, AF288600, AF288601, AF292942, AF301912, AF303659, AF303660, AF359461–AF359496, AJ009147–AJ009150, AJ620544, AY491762, AY785561–AY785586, M31432, and X53917 (84 *T. cruzi* SSU rDNA sequences), and AF065157, AJ009160, AJ012412–AJ012417, AY491766, and AY491767 (10 *T. rangeli* SSU rDNA sequences).

Phylogenetic analysis

For phylogenetic analyses, nucleotide sequences of SSU rDNA, 5.8S rDNA, and gGAPDH gene were examined. The newly obtained SSU rDNA sequence of the trypanosome, and those of related trypanosome species obtained from DDBJ/EMBL/GenBank, 1,828-bp to 2,233-bp long, were aligned using the CLUSTRAL W multiple alignment program, with subsequent manual adjustment. An insect trypanosomatid species, *Crithidia fasciculata*, was used as an outgroup. Regions judged to be poorly aligned, and characters with a gap in any sequence, were excluded from subsequent analyses; 1,703 characters, of which 312 were variable and 173 were parsimony-informative, remained for subsequent analyses. Phylogenetic analyses of the alignment were conducted using neighbor-joining (NJ), minimum evolution (ME), and maximum parsimony (MP) methods, as implemented in the MEGA program version 3.1 (Kumar et al., 2004). For all 3 methods, 1,000 bootstrap replicates were calculated.

To compare 5.8S rDNA, available sequences of *T. theileri* (AY773698–AY773700, AB007814), *T. cruzi* (M63701, L22334, AF362827–AF362829), *T. rangeli* (AY230232–AY230240, AF362832), *T. grosi* (AB175622–AB175624), *T. otospermophili* (AB175625, AB190228), *T. kuseli* (AB175626); 9 *Leishmania* spp. (AJ000306, AJ000311, AJ000313, AJ000314, AJ300484, AJ300485, AJ634371, AJ634372, AM502245, AJ634378, AY283793, DQ300180, DQ316038, DQ316039, DQ316052); and *Crithidia fasciculata* (Y00055) were obtained from the DDBJ/EMBL/GenBank and aligned by the CLUSTRAL W multiple alignment program. Regions judged to be poorly aligned, and characters with a gap in any sequence, were excluded from subsequent analyses; 163 characters, of which 12 were variable and 7 were parsimony-informative, remained for subsequent analyses. Based on the structural association between 5.8S and 28S rDNA (Hwang and Kim, 2000; Gottschling and Plötner, 2004), a putative secondary structure of the 5.8S rDNA of *T. minasense* was drawn, and base sites at which species-, subgenus-, or genus-specific substitutions constantly occur (parsimony-informative sites) were plotted on this 5.8S rDNA model to understand the structural basis for these changes.

For phylogenetic analyses based on the nucleotide sequences of the gGAPDH gene, the newly obtained sequence of the trypanosome, and those of related trypanosomatids obtained from DDBJ/EMBL/GenBank, were aligned using the CLUSTRAL W multiple alignment program, with subsequent manual adjustment. To convert nucleotide to amino acid sequences using the universal genetic code, the "translation tool" on the internet (http://ca.expasy.org/tools/dna.html) was used. According to Hamilton et al. (2004) and Hamilton, Stevens, Gildley et al (2005), the third codon position was excluded for analyses. Regions with a gap in any sequence were excluded from subsequent analyses; 387 characters, of which 107 were variable and 75 were parsimony-informative, remained for subsequent analyses. Phylogenetic analyses of the alignment were conducted as 18S rDNA analyses, mentioned above.

RESULTS

Prevalence of trypanosomes and their morphology

Peripheral blood of squirrel monkeys was drawn on 25 April 2005. A few trypanosomes were found in Giemsa-stained blood smears from 20 of the 85 squirrel monkeys (23.5%) by intensive microscopic examinations; in most cases, only a single trypomastigote was observed on a slide. As shown in Figure 1, trypanosomes from squirrel monkeys were pleiomorphic. They were, however, characterized by broad bodies with the anteriorly positioned kinetoplasts, coincident with the subgenus *Megatrypanum* (Hoare, 1972). Based on the host species, morphology, and morphometric data (Table I), the trypanosomes from squirrel monkeys were identified as *Trypanosoma* (*Megatrypanum*) *minasense* Chagas, 1909. PCR amplification of a highly variable region of the SSU rDNA was attempted with several blood samples using 4 primer combinations of TRY927F, TRY927R, SSU561F, and SSU561R; the primer pair of TRY927F and SSU561R succeeded in amplifying 650-bp long sequences of the trypanosomes in the blood of 4 squirrel monkeys. Except for 1 nucleotide, the sequence of these amplicons (DDBJ/EMBL/GenBank AB362412) was absolutely identical with that of trypanosomes from tamarins mentioned below.

On 11 November 2005, peripheral blood was taken from 15 tamarins, and buffy-coat examinations detected trypanosomes in 10 EDTA-treated blood samples (nos. 1–4, 6, 8, 10, 13, 15, and 16). On 6 January 2006, blood samples were collected from 15 tamarins, and buffy-coat examinations detected trypanosomes in 4 samples (nos. 8, 11, 12, and 15). On both occasions, trypanosomes were very few in number. PCR amplification of a highly variable region of trypanosome SSU rDNA detected the infection in 14 of the 15 tamarin blood samples taken on both occasions. As shown in Figure 2, PCR products of blood trypanosomes in 14 tamarins had identical molecular size, but smaller-than-calculated molecular sizes of the homologous region of 84 available *T. cruzi* sequences (999 bp–1,040 bp) or that of 10 available *T. rangeli* sequences (1,004 bp or 1,008 bp). Sequences of 4 arbitrarily chosen amplicons of 931-bp length by the primer pair of TRY927F and TRY927R were identical, indicating that infection by a single trypanosome species was prevalent in these tamarins, as in the squirrel monkeys mentioned above.

SSU/LSU rDNA of *T.* (*M.*) *minasense* and its molecular phylogenetic relationship with other trypanosomes

The rDNA sequences of *T. minasense* examined in the present study had 2,204-bp 18S, 449-bp ITS1, 172-bp 5.8S, more than 577-bp ITS2, 1,772-bp 28Sα, 49-bp ITS3, 214-bp 28Sγ, 78-bp ITS4, 1,484-bp 28Sβ, 52-bp ITS5, 183-bp 28Sδ, 193-bp ITS6, and more than 68-bp 28Sζ (DDBJ/EMBL/GenBank AB362411).

BLAST analysis of the newly obtained 2,196-bp sequence of 18S rDNA found *T. grayi* (a crocodile trypanosome in Africa) and *T. bennetti* (a kestrel trypanosome in North America) with the closest 18S sequences, followed by a variety of trypanosomes of the subgenus *Herpetosoma*, as well as trypanosome species having broad bodies, such as *T. avium* (an avian trypanosome) and *T. theileri* (a cattle trypanosome).

Bootstrap supports for partial topology were low in phylogenetic trees based on the SSU rDNA alignment of 21 named and several unnamed *Trypanosoma* spp., by either NJ, ME, or MP methods. There were apparently 4 groups in the constructed phylogenetic trees (Fig. 3): (1) *Megatrypanum*-type trypanosomes containing *T. theileri* clade, *T. avium* clade, and other trypanosomes of *T. theileri*-like morphology, (2) South American trypanosome clade containing *T. cruzi* and *T. rangeli*, (3) insectivore trypanosomes exhibiting *Megatrypanum* morphology, and (4) rodent trypanosome (the subgenus *Herpetosoma*) clade containing *T. lewisi* and trypanosomes with *T. lewisi*-like morphology. *Trypanosoma minasense* detected in the present study was in the *Megatrypanum*-type trypanosome group, close to *T. bennetti* and *T. grayi*.

5.8S rDNA of *T.* (*M.*) *minasense* and its molecular phylogenetic relationship with other trypanosomes

BLAST analysis of the newly obtained 172-bp sequence of 5.8S rDNA found *T. theileri* with the closest sequence, followed by *T. cruzi* rather than by *T. rangeli* or *Herpetosoma* trypanosomes. Limited numbers of deposited sequences of trypanosomes, other than SSU rDNA in the DDBJ/EMBL/GenBank, hampered further analyses.

The 5.8S rDNA alignment of 7 *Trypanosoma* spp. and 9 *Leishmania* spp. contained 7 parsimony-informative characters, which were mainly located at unpaired regions such as loop tips (Fig. 4). Table II compares nucleotides of different species at base positions of parsimony-informative or *Leishmania*-specific characters. The 5.8S rDNA sequences were rather consistent for a broad range of *Trypanosoma* spp. and *Leishmania* spp., but nucleotides unique to respective species (shown in Table II) were well conserved by multiple isolates, as determined from available sequences in the DDBJ/EMBL/GenBank. This suggested that *T. minasense* analyzed in the present study was distinct from *T. rangeli*.

gGAPDH genes of trypanosomes, in some blood samples, and their molecular phylogenetic relationships with reported trypanosome gGAPDH gene sequences

In a single round of PCR using a primer pair of G3 and G5, a specific band of 971-bp length was generated by a single blood sample from a tamarin (No. 15). Using the nested PCR after the first-round PCR, specific bands were obtained in blood samples of 2 squirrel monkeys (nos. 45, 54) and 3 tamarins (nos. 6, 10, 16). BLAST analyses of the 6 newly obtained sequences of gGAPDH gene (1 sequence of 971-bp length, 4 sequences of 883-bp length, and 1 sequence of 842-bp length) revealed either *T. rangeli* or *T. cruzi* as the closest sequence, rather than other trypanosome species.

The phylogenetic trees were constructed based on a gGAPDH gene alignment (the first and second codons) of fish, reptile, bird, and mammalian trypanosomes (Fig. 5). Relationships between different groups of trypanosomes were easily changed by the method used (NJ, ME, and MP), as evidenced by low bootstrap supports for partial topology in the proximal part of the phylogenetic tree. Regardless of tree construction, 2 sequences from 2 tamarins (nos. 10 and 16) grouped firmly with *T. cruzi*; 1 sequence from 1 tamarin (no. 6) and 2 squirrel monkeys (nos. 45 and 54) grouped with the LSTH isolate of *T.*